

organ-specific autoimmune diseases [33, 34]. However, IFN- $\gamma$  has recently been shown to be a down-regulatory cytokine, as evidenced by exacerbated myocarditis in IFN- $\gamma$  receptor knockout (KO), IFN- $\gamma$  KO, and T-bet KO mice [35–37]. On the other hand, Th17 cells have been implicated in the pathogenesis of various types of autoimmune diseases (reviewed in [38]); however, the genetic ablation of IL-17 had no significant impact on the incidence or severity of myocarditis [39]. These gene-ablated mice provided us with much important information, and we could not exclude the possibility that the inhibitory effect of pitavastatin on the IFN- $\gamma$  production may weaken the immunosuppressive effect of pitavastatin. However, studies from gene ablation mice do not necessarily match the results of the real world. We have previously reported that the suppressor of cytokine signaling 1 (SOCS1) DNA administration ameliorated EAM, and SOCS1 DNA therapy suppressed both Th1 and Th17 cytokines from CD4<sup>+</sup> T cells [10]. Ohshima et al. also reported that systemic transplantation of allogenic fetal membrane-derived mesenchymal stem cells suppresses both Th1 and Th17 T-cell responses in EAM [40]. The question of the relative roles of Th1 cells versus Th17 cells on EAM is unresolved [39, 41], and autoimmune diseases have so far been considered to be associated with both Th1 and Th17 cells [39, 42]. Statins can inhibit both Th1 and Th17 responses and may be a useful therapy for autoimmune diseases in the clinical setting.

As shown in Fig. 2a, a larger amount of pitavastatin was needed to inhibit STAT3 phosphorylation than was needed to inhibit STAT4 phosphorylation. Kagami et al. showed similar results that simvastatin inhibited the differentiation of Th17 cells at the concentrations that did not inhibit the differentiation of Th1 cells [43]. These findings suggest that statins can more easily affect the Th17 differentiation than affect the Th1 differentiation.

Several studies have shown that statins can modulate the inflammatory milieu by altering chemokines and chemokine receptors, eventually inhibiting the leukocyte migration [44, 45]. We evaluated the chemokine concentrations in the heart and found decreased levels of chemokines, including CCL2, CCL3, CCL5, CCL17, CCL20 and CXCL10 (Fig. 1e). We could not evaluate whether these decreases were direct effects of pitavastatin or not in our system, and this may have contributed to the beneficial effects of pitavastatin in EAM.

There are several reports of the effects of statins on inducing Tregs in humans. Atorvastatin treatment of human PBMCs in vitro led to an induction of the transcription factor Foxp3, accompanied by an increase in the number of Tregs [46]. Simvastatin and pravastatin treatment in hyperlipidemic patients increased the number of Tregs in PBMCs [46]. Tang et al. showed that atorvastatin promoted the generation of Tregs from primary T cells of rheumatoid arthritis patients [47]. On the other hand, there are some conflicting data on the

Treg induction by statins in mice. Consistent with our data (Fig. 2d), Mausner-Fainberg et al. did not find a statin-induced conversion of murine CD4<sup>+</sup>CD25<sup>+</sup>Foxp3<sup>+</sup> to Treg cells [46]. Mira et al. also demonstrated that no changes were noted in the Treg cell numbers in the spleen or draining lymph nodes of lovastatin-treated mice [48]. However, it has been reported that simvastatin increases the Treg differentiation in vitro [43, 49]. Thus, the question of the effect of statins on Tregs in mice is unresolved. It can be assumed that in murine models, the anti-inflammatory effects of pitavastatin are probably evident by inhibiting the Th1 and Th17 response rather than by the expansion of Tregs. Further studies are needed to elucidate the effect on the Treg induction in mice.

As a result of the HMG-CoA reductase inhibition, statins also inhibit the synthesis of downstream isoprenoids farnesyl-PP and geranylgeranyl-PP (Fig. 4a). The process of the isoprenylation of Ras/Rho family proteins is required for G protein activity. At least some of the pleiotropic benefits of statins that are independent of the cholesterol lowering effect are thought to involve interference with the normal synthesis of isoprenoids, thereby impairing the Ras/Rho G protein function (reviewed in ref. [50]). Dunn et al. showed that atorvastatin suppressed Th1 differentiation and caused a Th2 bias by inhibiting Ras farnesylation and RhoA geranylgeranylation [51]. Ras-ERK and RhoA-p38 signaling pathways are important in determination of Th1/Th2 fate [52–54]. In accordance with this evidence, our data have demonstrated that both inhibitors of farnesylation and geranylgeranylation prevented the Th1 differentiation (Fig. 4b and c). On the other hand, the Th17 differentiation was inhibited only by a farnesylation inhibitor (Fig. 4b and c). Recently, Rheb which belongs to the Ras family of G proteins [55] and downstream mammalian target of rapamycin (mTOR) signaling in T cells was shown to be necessary for Th1 and Th17 responses and the development of autoimmune disease [56]. Rheb-deficient T cells failed to differentiate into Th1 and Th17 cells, and mice with T cell-specific deletion of Rheb were resistant to the development of EAE [56]. Farnesylation of Rheb is necessary for its intracellular trafficking and subcellular localization to the plasma membrane and subsequent activation of the mTOR pathway [57]. Some in vitro studies have demonstrated an inhibitory effect of statin treatment on the farnesylation and membrane-association of Rheb [58, 59]. From our ongoing study, we have found that pitavastatin inhibited Rheb-mTOR signaling in a farnesylation-dependent manner (unpublished data). Collectively, these results suggest that pitavastatin prevents Th1 and Th17 differentiation by inhibiting the biosynthesis of farnesyl-PP, leading to reduced farnesylated Rheb and reduced downstream mTOR activity. Our data have demonstrated that both FTI-277 and GGTI-298 inhibited the Th1 differentiation, but Th17 differentiation was inhibited only by FTI-277 (Fig. 4). These results may have indicated that Th17 differentiation

is mainly regulated by farnesylated Rheb-mTOR signaling in our system, though Th1 differentiation is regulated not simply by farnesylated Rheb but also by other geranylgeranylated proteins. Further studies are needed to evaluate the mechanism.

In the present study, we have shown that both FTI-277 and GGTI-298 inhibited the Th1 differentiation, but the Th17 differentiation was inhibited mainly by FTI-277 (Fig. 4b and c). In contrast to our data, Kagami et al. reported that the inhibition of protein geranylgeranylation but not farnesylation is involved in the decreased differentiation of Th17 cells with simvastatin treatment [43]. There were some differences between their experiments and ours. They used a low-dose (5  $\mu$ M) of FTI-277 and GGTI-298 in their experiments, whereas we used a relatively high amount of those reagents (20  $\mu$ M). Therefore, we also checked the effects of low-dose FTI-277 and GGTI-298 on the Th differentiation and did not find any apparent effects on the Th differentiation (data not shown). Next, they used CD4<sup>+</sup>CD25<sup>-</sup> T cells for the Th skewing experiments, whereas we used CD4<sup>+</sup>CD62L<sup>+</sup> T cells. CD25 (IL-2 receptor  $\alpha$  chain) has been used as a marker for Tregs as well as activated T cells [60]. On the other hand, CD62L (L-selectin) is an important T-cell homing receptor as well as a marker for T-cell development. Naive T cells are CD62L<sup>+</sup>, and CD62L acts as a “homing receptor” for lymphocytes to enter secondary lymphoid tissues via high endothelial venules [61]. This difference may have influenced the results.

In conclusion, we have shown that pitavastatin inhibits CD4<sup>+</sup> T-cell proliferation and Th1/Th17 responses and ameliorates myocarditis in mice. Because oral statin administration is well tolerated, this treatment is a promising approach for the treatment of Th1- and Th17-mediated autoimmune diseases.

**Acknowledgments** We are grateful to Brian Purdue of the Medical English Communications Center of the University of Tsukuba for revising this manuscript. This work was supported by the University of Tsukuba Research Infrastructure Support Program.

**Conflict of Interest** The authors declare that they have no conflict of interest.

## References

1. Brown CA, O'Connell JB. Myocarditis and idiopathic dilated cardiomyopathy. *Am J Med.* 1995;99(3):309–14.
2. Caforio AL, Mahon NJ, Tona F, McKenna WJ. Circulating cardiac autoantibodies in dilated cardiomyopathy and myocarditis: pathogenetic and clinical significance. *Eur J Heart Fail.* 2002;4(4):411–7.
3. Lauer B, Schannwell M, Kuhl U, Strauer BE, Schultheiss HP. Antimyosin autoantibodies are associated with deterioration of systolic and diastolic left ventricular function in patients with chronic myocarditis. *J Am Coll Cardiol.* 2000;35(1):11–8.
4. Frustaci A, Chimenti C, Calabrese F, Pieroni M, Thiene G, Maseri A. Immunosuppressive therapy for active lymphocytic myocarditis: virological and immunologic profile of responders versus nonresponders. *Circulation.* 2003;107(6):857–63.
5. Caforio AL, Goldman JH, Haven AJ, Baig KM, Libera LD, McKenna WJ. Circulating cardiac-specific autoantibodies as markers of autoimmunity in clinical and biopsy-proven myocarditis. The Myocarditis Treatment Trial Investigators. *Eur Heart J.* 1997;18(2):270–5.
6. Fairweather D, Kaya Z, Shellam GR, Lawson CM, Rose NR. From infection to autoimmunity. *J Autoimmun.* 2001;16(3):175–86.
7. Neu N, Rose NR, Beisel KW, Herskowitz A, Gurri-Glass G, Craig SW. Cardiac myosin induces myocarditis in genetically predisposed mice. *J Immunol.* 1987;139(11):3630–6.
8. Eriksson U, Kurrer MO, Schmitz N, Marsch SC, Fontana A, Eugster HP, et al. Interleukin-6-deficient mice resist development of autoimmune myocarditis associated with impaired upregulation of complement C3. *Circulation.* 2003;107(2):320–5.
9. Eriksson U, Penninger JM. Autoimmune heart failure: new understandings of pathogenesis. *Int J Biochem Cell Biol.* 2005;37(1):27–32.
10. Tajiri K, Imanaka-Yoshida K, Matsubara A, Tsujimura Y, Hiroe M, Naka T, et al. Suppressor of cytokine signaling 1 DNA administration inhibits inflammatory and pathogenic responses in autoimmune myocarditis. *J Immunol.* 2012;189(4):2043–53.
11. Boekholdt SM, Arsenault BJ, Mora S, Pedersen TR, LaRosa JC, Nestel PJ, et al. Association of LDL cholesterol, non-HDL cholesterol, and apolipoprotein B levels with risk of cardiovascular events among patients treated with statins: a meta-analysis. *JAMA.* 2012;307(12):1302–9.
12. Ghittoni R, Lazzerini PE, Pasini FL, Baldari CT. T lymphocytes as targets of statins: molecular mechanisms and therapeutic perspectives. *Inflamm Allergy Drug Targets.* 2007;6(1):3–16.
13. Greenwood J, Walters CE, Pryce G, Kanuga N, Beraud E, Baker D, et al. Lovastatin inhibits brain endothelial cell Rho-mediated lymphocyte migration and attenuates experimental autoimmune encephalomyelitis. *FASEB J.* 2003;17(8):905–7.
14. Wang Y, Li D, Jones D, Bassett R, Sale GE, Khalili J, et al. Blocking LFA-1 activation with lovastatin prevents graft-versus-host disease in mouse bone marrow transplantation. *Biol Blood Marrow Transplant.* 2009;15(12):1513–22.
15. Aktas O, Waiczies S, Smorodchenko A, Dorr J, Seeger B, Prozorovski T, et al. Treatment of relapsing paralysis in experimental encephalomyelitis by targeting Th1 cells through atorvastatin. *J Exp Med.* 2003;197(6):725–33.
16. Youssef S, Stuve O, Patarroyo JC, Ruiz PJ, Radosevich JL, Hur EM, et al. The HMG-CoA reductase inhibitor, atorvastatin, promotes a Th2 bias and reverses paralysis in central nervous system autoimmune disease. *Nature.* 2002;420(6911):78–84.
17. Zhang X, Jin J, Peng X, Ramgolam VS, Markovic-Plese S. Simvastatin inhibits IL-17 secretion by targeting multiple IL-17-regulatory cytokines and by inhibiting the expression of IL-17 transcription factor RORC in CD4<sup>+</sup> lymphocytes. *J Immunol.* 2008;180(10):6988–96.
18. Sonderegger I, Iezzi G, Maier R, Schmitz N, Kurrer M, Kopf M. GM-CSF mediates autoimmunity by enhancing IL-6-dependent Th17 cell development and survival. *J Exp Med.* 2008;205(10):2281–94.
19. Valaperti A, Marty RR, Kania G, Germano D, Mauermann N, Dirnhofer S, et al. CD11b<sup>+</sup> monocytes abrogate Th17 CD4<sup>+</sup> T cell-mediated experimental autoimmune myocarditis. *J Immunol.* 2008;180(4):2686–95.
20. Eriksson U, Ricci R, Hunziker L, Kurrer MO, Oudit GY, Watts TH, et al. Dendritic cell-induced autoimmune heart failure requires cooperation between adaptive and innate immunity. *Nat Med.* 2003;9(12):1484–90.
21. Pinchuk LM, Filipov NM. Differential effects of age on circulating and splenic leukocyte populations in C57BL/6 and BALB/c male mice. *Immun Ageing.* 2008;5:1.

22. Cihakova D, Barin JG, Afanasyeva M, Kimura M, Fairweather D, Berg M, et al. Interleukin-13 protects against experimental autoimmune myocarditis by regulating macrophage differentiation. *Am J Pathol*. 2008;172(5):1195–208.
23. Darnell Jr JE. STATs and gene regulation. *Science*. 1997;277(5332):1630–5.
24. Yang XO, Panopoulos AD, Nurieva R, Chang SH, Wang D, Watowich SS, et al. STAT3 regulates cytokine-mediated generation of inflammatory helper T cells. *J Biol Chem*. 2007;282(13):9358–63.
25. Zhou L, Ivanov II, Spolski R, Min R, Shenderov K, Egawa T, et al. IL-6 programs T(H)-17 cell differentiation by promoting sequential engagement of the IL-21 and IL-23 pathways. *Nat Immunol*. 2007;8(9):967–74.
26. Shevach EM, DiPaolo RA, Andersson J, Zhao DM, Stephens GL, Thornton AM. The lifestyle of naturally occurring CD4<sup>+</sup> CD25<sup>+</sup> Foxp3<sup>+</sup> regulatory T cells. *Immunol Rev*. 2006;212:60–73.
27. Zheng Y, Rudensky AY. Foxp3 in control of the regulatory T cell lineage. *Nat Immunol*. 2007;8(5):457–62.
28. Szabo SJ, Kim ST, Costa GL, Zhang X, Fathman CG, Glimcher LH. A novel transcription factor, T-bet, directs Th1 lineage commitment. *Cell*. 2000;100(6):655–69.
29. Ivanov II, McKenzie BS, Zhou L, Tadokoro CE, Lepelley A, Lafaille JJ, et al. The orphan nuclear receptor ROR $\gamma$  directs the differentiation program of proinflammatory IL-17<sup>+</sup> T helper cells. *Cell*. 2006;126(6):1121–33.
30. Yang XO, Pappu BP, Nurieva R, Akimzhanov A, Kang HS, Chung Y, et al. T helper 17 lineage differentiation is programmed by orphan nuclear receptors ROR $\alpha$  and ROR $\gamma$ . *Immunity*. 2008;28(1):29–39.
31. Bergelson JM, Cunningham JA, Droguett G, Kurt-Jones EA, Krithivas A, Hong JS, et al. Isolation of a common receptor for Cocksackie B viruses and adenoviruses 2 and 5. *Science*. 1997;275(5304):1320–3.
32. Liu W, Li WM, Gao C, Sun NL. Effects of atorvastatin on the Th1/Th2 polarization of ongoing experimental autoimmune myocarditis in Lewis rats. *J Autoimmun*. 2005;25(4):258–63.
33. Gor DO, Rose NR, Greenspan NS. TH1-TH2: a procrustean paradigm. *Nat Immunol*. 2003;4(6):503–5.
34. Nishikubo K, Imanaka-Yoshida K, Tamaki S, Hiroe M, Yoshida T, Adachi Y, et al. Th1-type immune responses by Toll-like receptor 4 signaling are required for the development of myocarditis in mice with BCG-induced myocarditis. *J Autoimmun*. 2007;29(2–3):146–53.
35. Afanasyeva M, Wang Y, Kaya Z, Stafford EA, Dohmen KM, Sadighi Akha AA, et al. Interleukin-12 receptor/STAT4 signaling is required for the development of autoimmune myocarditis in mice by an interferon-gamma-independent pathway. *Circulation*. 2001;104(25):3145–51.
36. Eriksson U, Kurrer MO, Bingisser R, Eugster HP, Saremaslani P, Follath F, et al. Lethal autoimmune myocarditis in interferon-gamma receptor-deficient mice: enhanced disease severity by impaired inducible nitric oxide synthase induction. *Circulation*. 2001;103(1):18–21.
37. Rangachari M, Mauermann N, Marty RR, Dirnhofer S, Kurrer MO, Komnenovic V, et al. T-bet negatively regulates autoimmune myocarditis by suppressing local production of interleukin 17. *J Exp Med*. 2006;203(8):2009–19.
38. Ghoreschi K, Laurence A, Yang XP, Hirahara K, O'Shea JJ. T helper 17 cell heterogeneity and pathogenicity in autoimmune disease. *Trends Immunol*. 2011;32(9):395–401.
39. Baldeviano GC, Barin JG, Talor MV, Srinivasan S, Bedja D, Zheng D, et al. Interleukin-17A is dispensable for myocarditis but essential for the progression to dilated cardiomyopathy. *Circ Res*. 2010;106(10):1646–55.
40. Ohshima M, Yamahara K, Ishikane S, Harada K, Tsuda H, Otani K, et al. Systemic transplantation of allogenic fetal membrane-derived mesenchymal stem cells suppresses Th1 and Th17 T cell responses in experimental autoimmune myocarditis. *J Mol Cell Cardiol*. 2012;53(3):420–8.
41. Sonderegger I, Rohn TA, Kurrer MO, Iezzi G, Zou Y, Kastelein RA, et al. Neutralization of IL-17 by active vaccination inhibits IL-23-dependent autoimmune myocarditis. *Eur J Immunol*. 2006;36(11):2849–56.
42. Luger D, Silver PB, Tang J, Cua D, Chen Z, Iwakura Y, et al. Either a Th17 or a Th1 effector response can drive autoimmunity: conditions of disease induction affect dominant effector category. *J Exp Med*. 2008;205(4):799–810.
43. Kagami S, Owada T, Kanari H, Saito Y, Suto A, Ikeda K, et al. Protein geranylgeranylation regulates the balance between Th17 cells and Foxp3<sup>+</sup> regulatory T cells. *Int Immunol*. 2009;21(6):679–89.
44. Greenwood J, Steinman L, Zamvil SS. Statin therapy and autoimmune disease: from protein prenylation to immunomodulation. *Nat Rev Immunol*. 2006;6(5):358–70.
45. Kim TG, Byamba D, Wu WH, Lee MG. Statins inhibit chemotactic interaction between CCL20 and CCR6 in vitro: possible relevance to psoriasis treatment. *Exp Dermatol*. 2011;20(10):855–7.
46. Mausner-Fainberg K, Luboshits G, Mor A, Maysel-Auslender S, Rubinstein A, Keren G, et al. The effect of HMG-CoA reductase inhibitors on naturally occurring CD4<sup>+</sup>CD25<sup>+</sup> T cells. *Atherosclerosis*. 2008;197(2):829–39.
47. Tang TT, Song Y, Ding YJ, Liao YH, Yu X, Du R, et al. Atorvastatin upregulates regulatory T cells and reduces clinical disease activity in patients with rheumatoid arthritis. *J Lipid Res*. 2011;52(5):1023–32.
48. Mira E, Leon B, Barber DF, Jimenez-Baranda S, Goya I, Almonacid L, et al. Statins induce regulatory T cell recruitment via a CCL1 dependent pathway. *J Immunol*. 2008;181(5):3524–34.
49. Kim YC, Kim KK, Shevach EM. Simvastatin induces Foxp3<sup>+</sup> T regulatory cells by modulation of transforming growth factor-beta signal transduction. *Immunology*. 2010;130(4):484–93.
50. Liao JK, Laufs U. Pleiotropic effects of statins. *Annu Rev Pharmacol Toxicol*. 2005;45:89–118.
51. Dunn SE, Youssef S, Goldstein MJ, Prod'homme T, Weber MS, Zamvil SS, et al. Isoprenoids determine Th1/Th2 fate in pathogenic T cells, providing a mechanism of modulation of autoimmunity by atorvastatin. *J Exp Med*. 2006;203(2):401–12.
52. Jorritsma PJ, Brogdon JL, Bottomly K. Role of TCR-induced extracellular signal-regulated kinase activation in the regulation of early IL-4 expression in naive CD4<sup>+</sup> T cells. *J Immunol*. 2003;170(5):2427–34.
53. Badou A, Savignac M, Moreau M, Leclerc C, Foucras G, Cassar G, et al. Weak TCR stimulation induces a calcium signal that triggers IL-4 synthesis, stronger TCR stimulation induces MAP kinases that control IFN-gamma production. *Eur J Immunol*. 2001;31(8):2487–96.
54. Rincon M, Flavell RA. Reprogramming transcription during the differentiation of precursor CD4<sup>+</sup> T cells into effector Th1 and Th2 cells. *Microbes Infect*. 1999;1(1):43–50.
55. Aspuria PJ, Tamanoi F. The Rheb family of GTP-binding proteins. *Cell Signal*. 2004;16(10):1105–12.
56. Delgoffe GM, Pollizzi KN, Waickman AT, Heikamp E, Meyers DJ, Horton MR, et al. The kinase mTOR regulates the differentiation of helper T cells through the selective activation of signaling by mTORC1 and mTORC2. *Nat Immunol*. 2011;12(4):295–303.
57. Buerger C, DeVries B, Stambolic V. Localization of Rheb to the endomembrane is critical for its signaling function. *Biochem Biophys Res Commun*. 2006;344(3):869–80.

58. Wagner RJ, Martin KA, Powell RJ, Rzucidlo EM. Lovastatin induces VSMC differentiation through inhibition of Rheb and mTOR. *Am J Physiol Cell Physiol*. 2010;299(1):C119–27.
59. Finlay GA, Malhowski AJ, Liu Y, Fanburg BL, Kwiatkowski DJ, Toksoz D. Selective inhibition of growth of tuberous sclerosis complex 2 null cells by atorvastatin is associated with impaired Rheb and Rho GTPase function and reduced mTOR/S6 kinase activity. *Cancer Res*. 2007;67(20):9878–86.
60. Malek TR. The biology of interleukin-2. *Annu Rev Immunol*. 2008;26:453–79.
61. Butcher EC, Picker LJ. Lymphocyte homing and homeostasis. *Science*. 1996;272(5258):60–6.

## Dynamics of cellular immune responses in the acute phase of dengue virus infection

Tomoyuki Yoshida · Tsutomu Omatsu · Akatsuki Saito · Yuko Katakai · Yuki Iwasaki · Terue Kurosawa · Masataka Hamano · Atsunori Higashino · Shinichiro Nakamura · Tomohiko Takasaki · Yasuhiro Yasutomi · Ichiro Kurane · Hirofumi Akari

Received: 13 June 2012 / Accepted: 12 December 2012 / Published online: 5 February 2013  
© Springer-Verlag Wien 2013

**Abstract** In this study, we examined the dynamics of cellular immune responses in the acute phase of dengue virus (DENV) infection in a marmoset model. Here, we found that DENV infection in marmosets greatly induced responses of CD4/CD8 central memory T and NKT cells. Interestingly, the strength of the immune response was greater in animals infected with a dengue fever strain than in those infected with a dengue hemorrhagic fever strain of DENV. In contrast, when animals were re-challenged with the same DENV strain used for primary infection, the neutralizing antibody induced appeared to play a critical role in sterilizing inhibition against viral replication, resulting in strong but delayed responses of CD4/CD8 central memory T and NKT cells. The results in this study may help to better understand the dynamics of cellular and humoral immune responses in the control of DENV infection.

T. Yoshida and T. Omatsu contributed equally to this study.

**Electronic supplementary material** The online version of this article (doi:10.1007/s00705-013-1618-6) contains supplementary material, which is available to authorized users.

T. Yoshida · Y. Iwasaki · T. Kurosawa · M. Hamano · Y. Yasutomi · H. Akari  
Tsukuba Primate Research Center, National Institute of Biomedical Innovation, 1-1 Hachimandai, Tsukuba, Ibaraki 305-0843, Japan

T. Yoshida (✉) · A. Saito · A. Higashino · H. Akari (✉)  
Center for Human Evolution Modeling Research,  
Primate Research Institute, Kyoto University, Inuyama,  
Aichi 484-8506, Japan  
e-mail: yoshida.tomoyuki.4w@kyoto-u.ac.jp

H. Akari  
e-mail: akari.hirofumi.5z@kyoto-u.ac.jp

### Introduction

Dengue virus (DENV) causes the most prevalent arthropod-borne viral infections in the world [29]. Infection with one of the four serotypes of DENV can lead to dengue fever (DF) and sometimes to fatal dengue hemorrhagic fever (DHF) or dengue shock syndrome (DSS) [12]. The serious diseases are more likely to develop after secondary infection with a serotype of DENV that is different from that of the primary infection. Infection with DENV induces a high-titered neutralizing antibody response that can provide long-term immunity to the homologous DENV serotype, while the effect of the antibody on the heterologous serotypes is transient [22]. On the other hand, enhanced pathogenicity after secondary DENV infection appears to be explained by antibody-dependent enhancement (ADE). Mouse and monkey experiments have shown that sub-neutralizing levels of DENV-specific antibodies actually enhance infection [1, 6, 11]. Thus, the development of an effective tetravalent dengue vaccine is considered to be an important public-health priority. Recently, several DENV vaccine candidates have undergone clinical trials, and most of them target the induction of neutralizing antibodies [20].

T. Omatsu · T. Takasaki · I. Kurane  
Department of Virology I, National Institute of Infectious Diseases, 1-23-1 Toyama, Shinjuku-ku, Tokyo 162-8640, Japan

Y. Katakai  
Corporation for Production and Research of Laboratory Primates, 1-1 Hachimandai, Tsukuba, Ibaraki 305-0843, Japan

S. Nakamura  
Research Center for Animal Life Science,  
Shiga University of Medical Science, Seta Tsukinowa-cho,  
Otsu, Shiga 520-2192, Japan

Research of the long-term immune response in humans has provided several interesting parallels to the data. It was reported that complete cross-protective immunity from heterologous challenge was induced in individuals 1–2 months after a primary DENV infection, with partial immunity present up to 9 months, resulting in a milder disease of shorter duration on reinfection, and that complete serotype-specific immunity against symptomatic dengue was observed up to 18 months postinfection [30]. Guzman and Sierra have previously recorded the long-term presence of both DENV-specific antibodies and T cells up to 20 years after natural infections [10, 31]. Of note, increased T cell activation is reportedly associated with severe dengue disease [7, 8]. Thus, the balance between humoral and cellular immunity may be important in the control of dengue diseases.

However, the details regarding the implication of humoral and cellular immunity in controlling DENV infection remain to be elucidated. Previously, passive transfer of either monoclonal or polyclonal antibodies was shown to protect against homologous DENV challenge [13, 15, 16]. It was also reported that neutralizing antibodies played a greater role than cytotoxic T lymphocyte (CTL) responses in heterologous protection against secondary DENV infection *in vivo* in IFN- $\alpha$ / $\beta$ R $^{-/-}$  and IFN $\gamma$ R $^{-/-}$  mouse models [18]. Moreover, CD4 $^{+}$  T cell depletion did not affect the DENV-specific IgG or IgM Ab titers or their neutralizing activity in the IFN $\gamma$ R $^{-/-}$  mouse model [36]. On the other hand, there are several reports showing that cellular immunity rather than humoral immunity plays an important role in the clearance of DENV. For example, in adoptive transfer experiments, although cross-reactive DENV-1-specific CD8 $^{+}$  T cells did not mediate protection against a lethal DENV-2 infection, adoptive transfer of CD4 $^{+}$  T cells alone mediated protection and delayed mortality in IFN- $\alpha$ / $\beta$ R $^{-/-}$  and IFN $\gamma$ R $^{-/-}$  mouse models [39]. It has also been demonstrated that CD8 $^{+}$  T lymphocytes have a direct role in protection against DENV challenge in the IFN- $\alpha$ / $\beta$ R $^{-/-}$  mouse model of DENV infection by depleting CD8 $^{+}$  T cells [35]. In addition, previous data from adoptive-transfer experiments in BALB/c mice showed that cross-reactive memory CD8 $^{+}$  T cells were preferentially activated by the secondary DENV infection, resulting in augmented IFN- $\gamma$  and tumor necrosis factor- $\alpha$  (TNF- $\alpha$ ) responses, and this effect was serotype-dependent [2, 3]. Although it has previously been suggested that inducing neutralizing antibodies against DENV may play an important role in controlling DENV infection, CTLs are also proposed to contribute to clearance during primary DENV infection and to pathogenesis during secondary heterologous infection in the BALB/c mouse model [4].

Why did the mouse models of DENV infection show inconsistent results *in vivo*? One of the reasons could be

that these results were obtained mainly from genetically manipulated mice such as IFN- $\alpha$ / $\beta$ R $^{-/-}$  and IFN $\gamma$ R $^{-/-}$  mice. Moreover, these mice were inoculated with  $10^9$ – $10^{10}$  genome equivalents (GE) of DENV [27, 35, 36], which were likely in large excess compared with the  $10^4$ – $10^5$  GE of DENV injected into humans by a mosquito [19]. In addition, the efficiency of DENV replication in wild mice *in vivo* is very low compared to that in humans [35].

Recently, novel non-human primate models of DENV infection using rhesus macaques as well as marmosets and tamarins have been developed [24–26, 38]. An intravenous challenge of rhesus macaques with a high dose of virus inoculum ( $1 \times 10^7$  GE) of DENV-2 resulted in readily visible hemorrhaging, which is one of the cardinal symptoms of human DHF [26]. It was also shown that the cellular immune response was activated due to expression of IFN- $\gamma$ , TNF- $\alpha$ , and macrophage inflammatory protein-1  $\beta$  in CD4 $^{+}$  and CD8 $^{+}$  T cells during primary DENV infection in rhesus macaques [20]. On the other hand, in the marmoset model of DENV infection, we observed high levels of viremia ( $10^5$ – $10^7$  GE/ml) after subcutaneous inoculation with  $10^4$ – $10^5$  plaque-forming units (PFU) of DENV-2. Moreover, we demonstrated that DENV-specific IgM and IgG were consistently detected and that the DENV-2 genome was not detected in any of these marmosets inoculated with the same DENV-2 strain used in the primary infection [24]. It is notable that while neutralizing antibody titers were at levels of 1:20–1:80 before the re-challenge inoculation, the titers increased up to 1:160–1:640 after the re-challenge inoculation [24]. These results suggested that the secondary infection with DENV-2 induced a protective humoral immunity to DENV-2 and that DENV-infected marmoset models may be useful in order to analyze the relationship between DENV replication and the dynamics of adaptive immune responses *in vivo*.

Taking these findings into consideration, we investigated the dynamics of cellular immunity in response to primary and secondary DENV infection in the marmoset model.

## Materials and methods

### Animals

All animal studies were conducted in accordance with protocols of experimental procedures that were approved by the Animal Welfare and Animal Care Committee of the National Institute of Infectious Diseases, Japan, and the National Institute of Biomedical Innovation, Japan. A total of six male marmosets, weighing 258–512 g, were used. Common marmosets were purchased from Clea Japan Inc.

(Tokyo, Japan) and caged singly at  $27 \pm 2^\circ\text{C}$  in  $50 \pm 10\%$  humidity with a 12-h light-dark cycle (lighting from 7:00 to 19:00) at Tsukuba Primate Research Center, National Institute of Biomedical Innovation, Tsukuba, Japan. Animals were fed twice a day with a standard marmoset diet (CMS-1M, CLEA Japan) supplemented with fruit, eggs and milk. Water was given ad libitum. The animals were in healthy condition and confirmed to be negative for anti-dengue-virus antibodies before inoculation with dengue virus [24].

Cells

Cell culture was performed as described previously [24]. Vero cells were cultured in minimum essential medium (MEM, Sigma) with 10 % heat-inactivated fetal bovine

serum (FBS, GIBCO) and 1 % non-essential amino acid (NEAA, Sigma) at  $37^\circ\text{C}$  in 5 %  $\text{CO}_2$ . C6/36 cells were cultured in MEM with 10 % FBS and 1 % NEAA at  $28^\circ\text{C}$  in 5 %  $\text{CO}_2$ .

Virus

DENV type 2 (DENV-2) strain DHF0663 (accession no. AB189122) and strain D2/Hu/Maldives/77/2008NIID (Mal/77/08) were used for inoculation studies. The DENV-2, DHF0663 strain was isolated from a DHF case in Indonesia. The DENV-2 Mal/77/08 strain was isolated from imported DF cases from the Maldives. For all DENV strains, isolated clinical samples were propagated in C6/36 cells and were used within four passages on C6/36 cells. Culture supernatant from infected C6/36 cells was

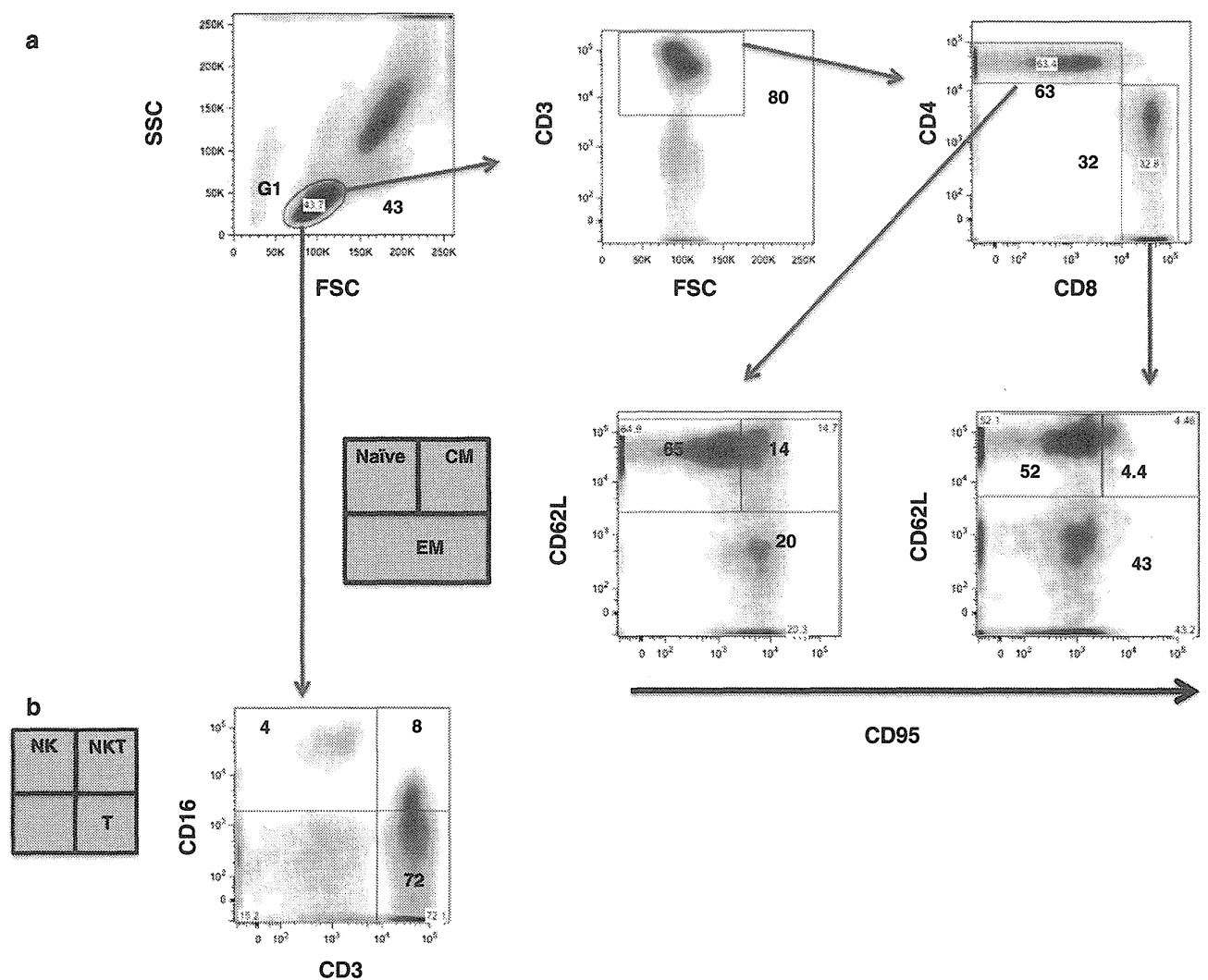


**Fig. 1** Flow cytometric analysis of naïve, central/effecter memory T cells and NK/NKT cells in marmosets. (a) Gating strategy to identify CD4 and CD8 T, NK and NKT cells. The G1 population was selected and analyzed for CD4 and CD8 T, NK and NKT cells. (b) Profiling of NK and NKT cells in total lymphocytes. Results shown are representative of three healthy marmosets used in this study

centrifuged at 3,000 rpm for 5 min to remove cell debris and then stored at  $-80\text{ }^{\circ}\text{C}$  until use.

Infection of the marmosets with DENV

In the challenge experiments, profiling of the key adaptive and innate immune cells in the marmosets after infection with DENV-2 was done. For primary DENV infection, four marmosets were inoculated subcutaneously in the back with either  $1.9 \times 10^5$  PFU of the DENV-2 Mal/77/08 strain (Cj08-007, Cj07-011) or  $1.8 \times 10^4$  PFU of the DHF0663 strain (Cj07-006, Cj07-008) [24]. In the case of the DENV re-challenge experiment, two marmosets initially inoculated with  $1.8 \times 10^5$  PFU of the DHF0663 strain were re-inoculated 33 weeks after the primary challenge with  $1.8 \times 10^5$  PFU of the same strain (Cj07-007, Cj07-014) [24]. Blood samples were collected on days 0, 1, 3, 7, 14, and 21 after inoculation and were used for virus titration and flow cytometric analysis. Inoculation with DENV and blood drawing were performed under anesthesia with 5 mg/kg of ketamine hydrochloride. Day 0 was defined as the day of virus inoculation. The viral loads in marmosets obtained in a previous study are shown in Supplementary Figure 1 [24].

Flow cytometry

Flow cytometry was performed as described previously [37]. Fifty microliters of whole blood from marmosets was stained with combinations of fluorescence-conjugated monoclonal antibodies; anti-CD3 (SP34-2; Becton Dickinson), anti-CD4 (L200; BD Pharmingen), anti-CD8 (CLB-T8/4H8; Sanquin), anti-CD16 (3G8; BD Pharmingen), anti-CD95 (DX2; BD Pharmingen), and anti-CD62L (145/15; Miltenyi Biotec). Then, erythrocytes were lysed with

FACS lysing solution (Becton Dickinson). After washing with a sample buffer containing phosphate-buffered saline (PBS) and 1 % FBS, the labeled cells were resuspended in a fix buffer containing PBS and 1 % formaldehyde. The expression of these markers on the lymphocytes was analyzed using a FACSCanto II flow cytometer (Becton Dickinson). The data analysis was conducted using FlowJo software (Treestar, Inc.). Results are shown as mean  $\pm$  standard deviation (SD) for the marmosets used in this study.

Results

Naïve central/effector memory T cells and NK/NKT cells in marmosets

Basic information regarding CD4/CD8 naïve and central/effector memory T cells and NK/NKT cells in common marmosets was unavailable. Thus, we examined the immunophenotypes of lymphocyte subsets in the marmosets (Fig. 1). The gating strategy for profiling the CD4 and CD8 T cells in the marmosets by FACS is shown in Fig. 1a. Human T cells are classically divided into three functional subsets based on their cell-surface expression of CD62L and CD95, i.e., CD62L<sup>+</sup>CD95<sup>-</sup> naïve T cells (T<sub>N</sub>), CD62L<sup>+</sup>CD95<sup>+</sup> central memory T cells (T<sub>CM</sub>), and CD62L<sup>-</sup>CD95<sup>±</sup> effector memory T cells (T<sub>EM</sub>) [9, 21, 28]. In this study, CD4<sup>+</sup> and CD8<sup>+</sup> T<sub>N</sub>, T<sub>CM</sub>, and T<sub>EM</sub> subpopulations were defined as CD62L<sup>+</sup>CD95<sup>-</sup>, CD62L<sup>+</sup>CD95<sup>+</sup>, and CD62L<sup>-</sup>CD95<sup>±</sup>, respectively (Fig. 1a and Table 1). The average ratio of CD3<sup>+</sup> T lymphocytes in the total lymphocytes of three marmosets was found to be  $75.7 \pm 6.4\%$ . The average ratio of CD4<sup>+</sup> T cells in the CD3<sup>+</sup> subset was  $65.4 \pm 6.8\%$ . The average ratios of CD4<sup>+</sup> T<sub>N</sub>, T<sub>CM</sub>, and T<sub>EM</sub> cells were  $65.9 \pm 3.7\%$ ,  $16.4 \pm 2.9\%$ ,  $19.5 \pm 2.5\%$ , respectively. The average ratio of CD8<sup>+</sup> T cells in the CD3<sup>+</sup> subset was  $29.0 \pm 8.0\%$ . The average ratios of CD8<sup>+</sup> T<sub>N</sub>, T<sub>CM</sub>, and T<sub>EM</sub> cells were  $66.7 \pm 10.2\%$ ,  $4.7 \pm 3.6\%$ ,  $28.8 \pm 14.8\%$ , respectively.

We recently characterized a CD16<sup>+</sup> major NK cell subset in tamarins and compared NK activity in tamarins with or without DENV infection [37, 38]. In terms of NKT cells, NK1.1 (CD161) and CD1d are generally used as markers of NKT cells [32]. However, these anti-human NK1.1 and CD1d antibodies are unlikely to cross-react with the NKT cells of the marmosets. Thus, we defined NKT cells as a population expressing both CD3 and CD16 as reported previously [14, 17]. The NK and NKT cell subsets were determined to be CD3<sup>-</sup>CD16<sup>+</sup> and CD3<sup>+</sup>CD16<sup>+</sup> lymphocytes in the marmosets. The average ratios of NK and NKT cell subsets in the lymphocytes were  $4.2 \pm 2.6\%$  and  $5.1 \pm 3.4\%$ , respectively (Table 1). We observed that the proportions of the major lymphocyte

Table 1 Subpopulation ratios of lymphocytes in marmosets	
Subpopulation name	Subpopulation ratios (Mean $\pm$ SD: %)
CD3 <sup>+</sup>	75.7 $\pm$ 6.4
CD3 <sup>+</sup> CD4 <sup>+</sup>	65.4 $\pm$ 6.8
CD3 <sup>+</sup> CD4 <sup>+</sup> CD62L <sup>+</sup> CD95 <sup>-</sup> (CD4 T <sub>N</sub> )	65.9 $\pm$ 3.7
CD3 <sup>+</sup> CD4 <sup>+</sup> CD62L <sup>+</sup> CD95 <sup>+</sup> (CD4 T <sub>CM</sub> )	16.4 $\pm$ 2.9
CD3 <sup>+</sup> CD4 <sup>+</sup> CD62LCD95 <sup>±</sup> (CD4 T <sub>EM</sub> )	19.5 $\pm$ 2.5
CD3 <sup>+</sup> CD8 <sup>+</sup>	29.0 $\pm$ 8.0
CD3 <sup>+</sup> CD8 <sup>+</sup> CD62L <sup>+</sup> CD95 <sup>-</sup> (CD8 T <sub>N</sub> )	66.7 $\pm$ 10.2
CD3 <sup>+</sup> CD8 <sup>+</sup> CD62L <sup>+</sup> CD95 <sup>+</sup> (CD8 T <sub>CM</sub> )	4.7 $\pm$ 3.6
CD3 <sup>+</sup> CD8 <sup>+</sup> CD62LCD95 <sup>±</sup> (CD8 T <sub>EM</sub> )	28.8 $\pm$ 14.8
CD3CD16 <sup>+</sup> (NK)	4.2 $\pm$ 2.6
CD3 <sup>+</sup> CD16 <sup>+</sup> (NKT)	5.1 $\pm$ 3.4

SD: Standard deviation  
Results shown are mean  $\pm$  SD from 3 healthy marmosets

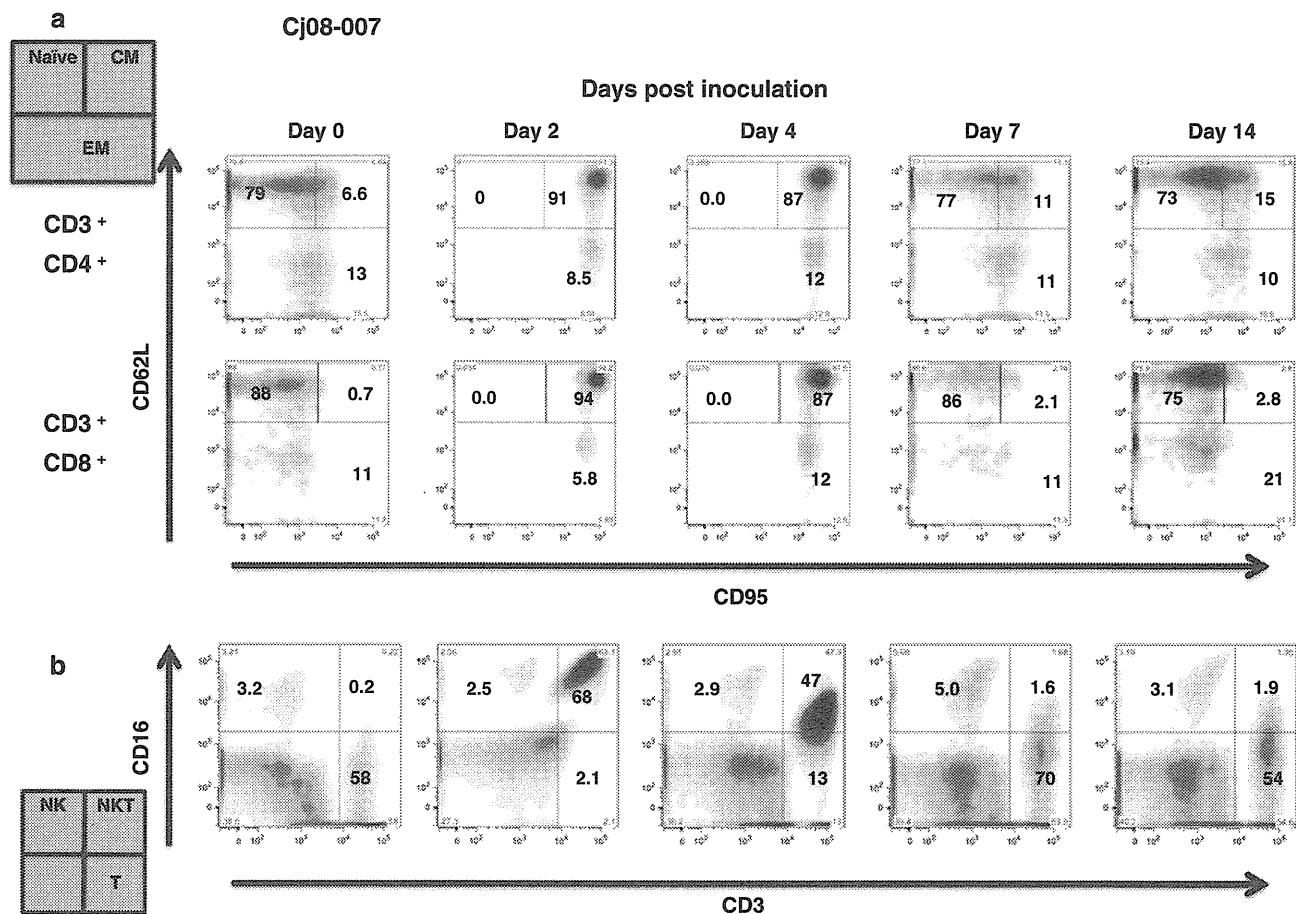


**Fig. 2 Profiling of CD4 and CD8 T, NK and NKT cells in marmosets with primary infection with the DENV-2 Mal/77/08 strain.** For primary DENV infection, two marmosets were inoculated subcutaneously in the back with  $1.9 \times 10^5$  PFU of the DENV-2 Mal/77/08 strain. (a) Profiling of naïve, central memory, and effector memory CD4 and CD8 T cells in total CD4 and CD8 T cells. (b) Profiling of NK and NKT cells in total lymphocytes. (a–b) Cj08-007

subsets in the marmosets were similar to those in cynomolgus monkeys and tamarins [37, 38].

Profiling of CD4 and CD8 T, NK and NKT cells in marmosets after primary infection with DENV-2 (Mal/77/08 strain)

We investigated the cellular immune responses against DENV-2 DF strain (Mal/77/08) in marmosets. Dengue vRNA was detected in plasma samples from two marmosets on day 2 postinfection (Supplementary Fig. 1a). For the two marmosets (Cj08-007, Cj07-011), the plasma levels of vRNA reached their peaks at  $9.6 \times 10^6$  and  $7.0 \times 10^6$  GE/ml, respectively, on day 4 postinfection. Plasma vRNA was detected in both marmosets on days 2, 4, and 7. We then examined the profiles and frequencies of the CD4 and CD8 T, NK and NKT cells in the infected marmosets (Figs. 2–3 and Table 2). CD4<sup>+</sup> T<sub>CM</sub> cells drastically increased to  $88.7 \pm 2.8$  % from  $13 \pm 0.4$  % between day 0 and day 2 post-inoculation (Table 2). Reciprocally,

CD4<sup>+</sup> T<sub>N</sub> cells decreased to  $1.6 \pm 3.3$  % from  $74.1 \pm 0.9$  % at the same time. CD4<sup>+</sup> T<sub>EM</sub> cells maintained the initial levels throughout the observation period. CD8<sup>+</sup> T<sub>CM</sub> cells increased to  $91.9 \pm 5.5$  % from  $2.1 \pm 0.8$  % between day 0 day 2 post-inoculation, and reciprocally, CD8<sup>+</sup> T<sub>N</sub> cells decreased to  $2.5 \pm 4.7$  % from  $89.9 \pm 2.5$  % at the same time. In addition, NK cells maintained their initial levels throughout the observation period. However, NKT cells drastically increased to  $52.6 \pm 17$  % from  $0.2 \pm 0.0$  % between day 0 and day 2 post-inoculation. These results suggest that CD4/CD8 T and NKT cells may efficiently respond to the Mal/77/08 strain of DENV.

Profiling of CD4 and CD8 T, NK and NKT cells in the marmosets after primary infection with DENV-2 (DHF0663 strain)

Next, we investigated cellular immune responses against another DENV-2 DHF strain (DHF0663) in marmosets.

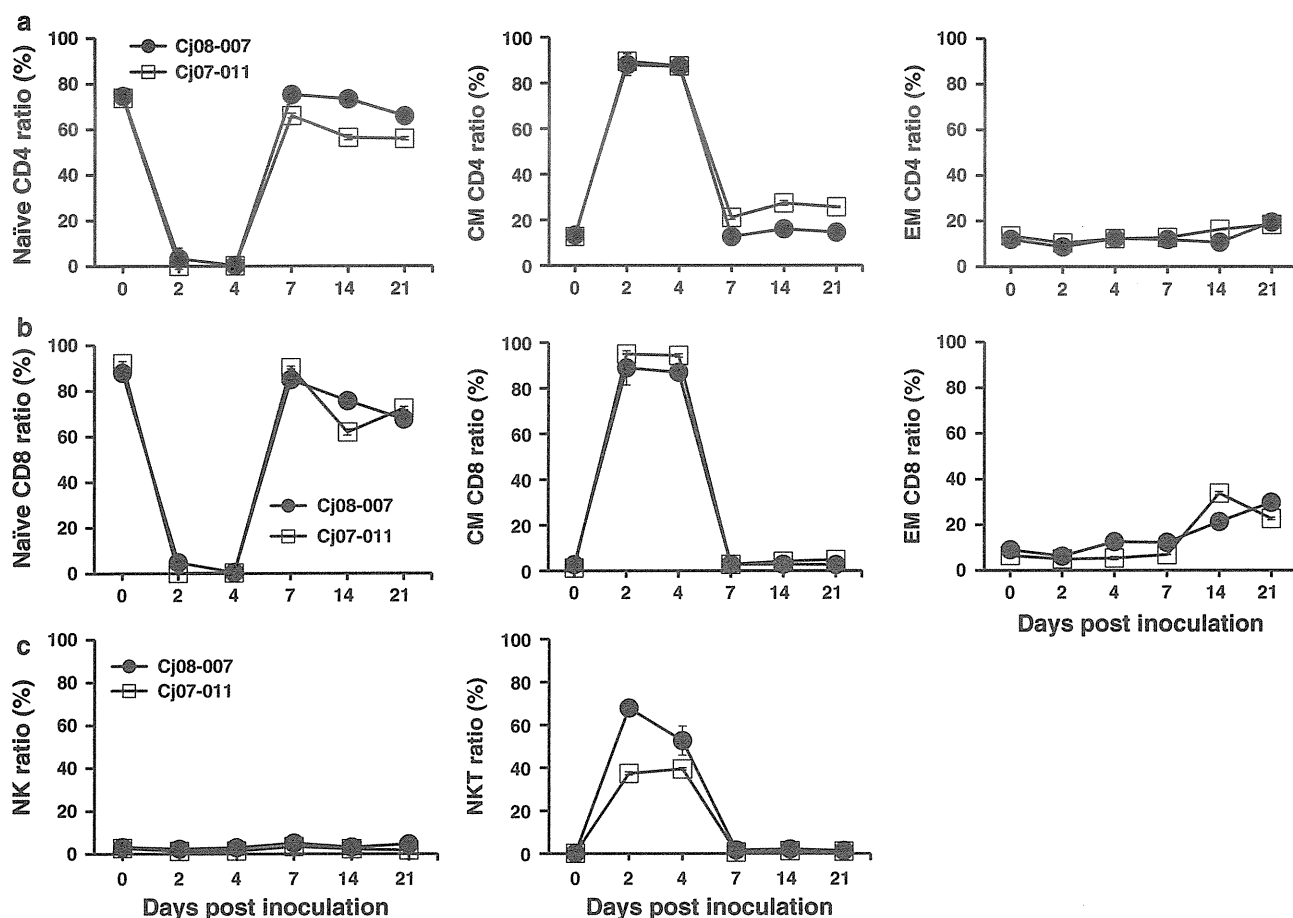


**Fig. 3** Frequency of CD4 and CD8 T, NK and NKT cells in marmosets with primary infection with the DENV-2 Mal/77/08 strain. For primary DENV infection, two marmosets were inoculated subcutaneously in the back with  $1.9 \times 10^5$  PFU of the DENV-2 Mal/77/08 strain. (a) Ratios of naïve, central memory, and effector

memory CD4 T cells in total CD4 T cells. (b) Ratios of naïve, central memory, and effector memory CD8 T cells in total CD8 T cells. (c) Ratios of NK and NKT cells in total lymphocytes. (a-c) Cj08-007, Cj07-011

**Table 2** Subpopulation ratios of lymphocytes in marmosets during primary DENV infection (Mal/77/08)

Subpopulation name		Subpopulation ratio (Mean $\pm$ SD: %)					
		Days after inoculation					
		Day 0	Day 2	Day 4	Day 7	Day 14	Day 21
CD3 <sup>+</sup> CD4 <sup>+</sup> CD62L <sup>+</sup> CD95 <sup>hi</sup>	(CD4 T <sub>N</sub> )	74.1 $\pm$ 0.9	1.6 $\pm$ 3.3	0.2 $\pm$ 0.3	70.5 $\pm$ 5.5	64.8 $\pm$ 9.7	60.8 $\pm$ 5.9
CD3 <sup>+</sup> CD4 <sup>+</sup> CD62L <sup>+</sup> CD95 <sup>+</sup>	(CD4 T <sub>CM</sub> )	13 $\pm$ 0.4	88.7 $\pm$ 2.8	87.4 $\pm$ 0.2	16.8 $\pm$ 5.0	21.6 $\pm$ 6.5	20 $\pm$ 6.4
CD3 <sup>+</sup> CD4 <sup>+</sup> CD62LCD95 <sup>+</sup>	(CD4 T <sub>EN</sub> )	12.8 $\pm$ 0.9	9.5 $\pm$ 1.0	12.3 $\pm$ 0.4	12.3 $\pm$ 0.5	134 $\pm$ 3.2	189 $\pm$ 1.4
CD3 <sup>+</sup> CD8 <sup>+</sup> CD62L <sup>+</sup> CD95 <sup>hi</sup>	(CD8 T <sub>N</sub> )	89.9 $\pm$ 2.5	2.5 $\pm$ 4.7	0.3 $\pm$ 0.3	87.5 $\pm$ 3.3	68.7 $\pm$ 79	69.8 $\pm$ 3.1
CD3 <sup>+</sup> CD8 <sup>+</sup> CD62L <sup>+</sup> CD95 <sup>+</sup>	(CD8 T <sub>CM</sub> )	2.1 $\pm$ 0.8	91.9 $\pm$ 5.5	90.6 $\pm$ 4.2	2.8 $\pm$ 0.5	3.5 $\pm$ 08	3.8 $\pm$ 1.2
CD3 <sup>+</sup> CD8 <sup>+</sup> CD62LCD95 <sup>+</sup>	(CD8 T <sub>EN</sub> )	7.8 $\pm$ 1.6	5.6 $\pm$ 0.8	9.0 $\pm$ 4.1	9.5 $\pm$ 3.1	27.6 $\pm$ 72	26.3 $\pm$ 4.3
CD3 <sup>+</sup> CD16 <sup>+</sup>	(NK)	2.9 $\pm$ 0.2	1.8 $\pm$ 0.6	2.2 $\pm$ 0.9	4.2 $\pm$ 0.9	2.8 $\pm$ 04	3.2 $\pm$ 1.7
CD3 <sup>+</sup> CD16 <sup>+</sup>	(NKT)	0.2 $\pm$ 0.0	52.6 $\pm$ 17	46.1 $\pm$ 8.5	1.1 $\pm$ 05	1.7 $\pm$ 05	1.2 $\pm$ 0.2

SD: Standard deviation

Results shown are mean  $\pm$  SD from two marmosets as shown in Figure 3

Dengue vRNA was detected in plasma samples from the marmosets on day 2 post-infection ([24], Supplementary Fig. 1b). For the two marmosets (Cj07-006, Cj07-008), the plasma vRNA levels were found to be  $3.4 \times 10^5$  and  $3.8 \times 10^5$  GE/ml on day 2 and  $2.0 \times 10^6$  and  $9.4 \times 10^5$  GE/ml, respectively, at the peak on day 4 post-infection and became undetectable by day 14. Thus, we examined the profiles and frequencies of the CD4<sup>+</sup> and CD8<sup>+</sup> T, NK and NKT cells in these DENV-infected marmosets (Fig. 4–5 and Table 3). It was found that on day 7 post-inoculation, CD4<sup>+</sup> and CD8<sup>+</sup> T<sub>N</sub> cells decreased, and in contrast, the T<sub>CM</sub> populations increased in both marmosets; however, the changes in proportion were much less pronounced than in the case of the marmosets infected with the DF strain. We observed no consistent tendency in the kinetics of CD4<sup>+</sup> and CD8<sup>+</sup> T<sub>EM</sub> cells nor in NK and NKT cells. These results suggest that the strength of T cell responses may be dependent on the strain of DENV.

Profiling of CD4 and CD8 T, NK and NKT cells in marmosets re-challenged with a DENV-2 strain

In order to examine the cellular immune responses against re-challenge with a DENV-2 DHF strain in the marmoset model, marmosets were infected twice with the same DENV-2 strain (DHF0663) with an interval of 33 weeks after the primary infection. The results showed that vRNA and NS1 antigens were not detected in plasma and that the neutralizing antibody titer was obviously increased after the secondary infection. The data indicated that the primary infection induced protective immunity, including a neutralizing antibody response to re-challenge with the same DENV strain ([24]; Supplementary Fig. 1c). We also investigated the profiles of the CD4 and CD8 T, NK and NKT cells in the marmosets (Cj07-007, Cj07-014) that were re-challenged with the same DENV-2 strain (DHF0663) (Figs. 6–7). CD4<sup>+</sup> T<sub>CM</sub> cells drastically increased on day 14 post-inoculation. On the other hand,

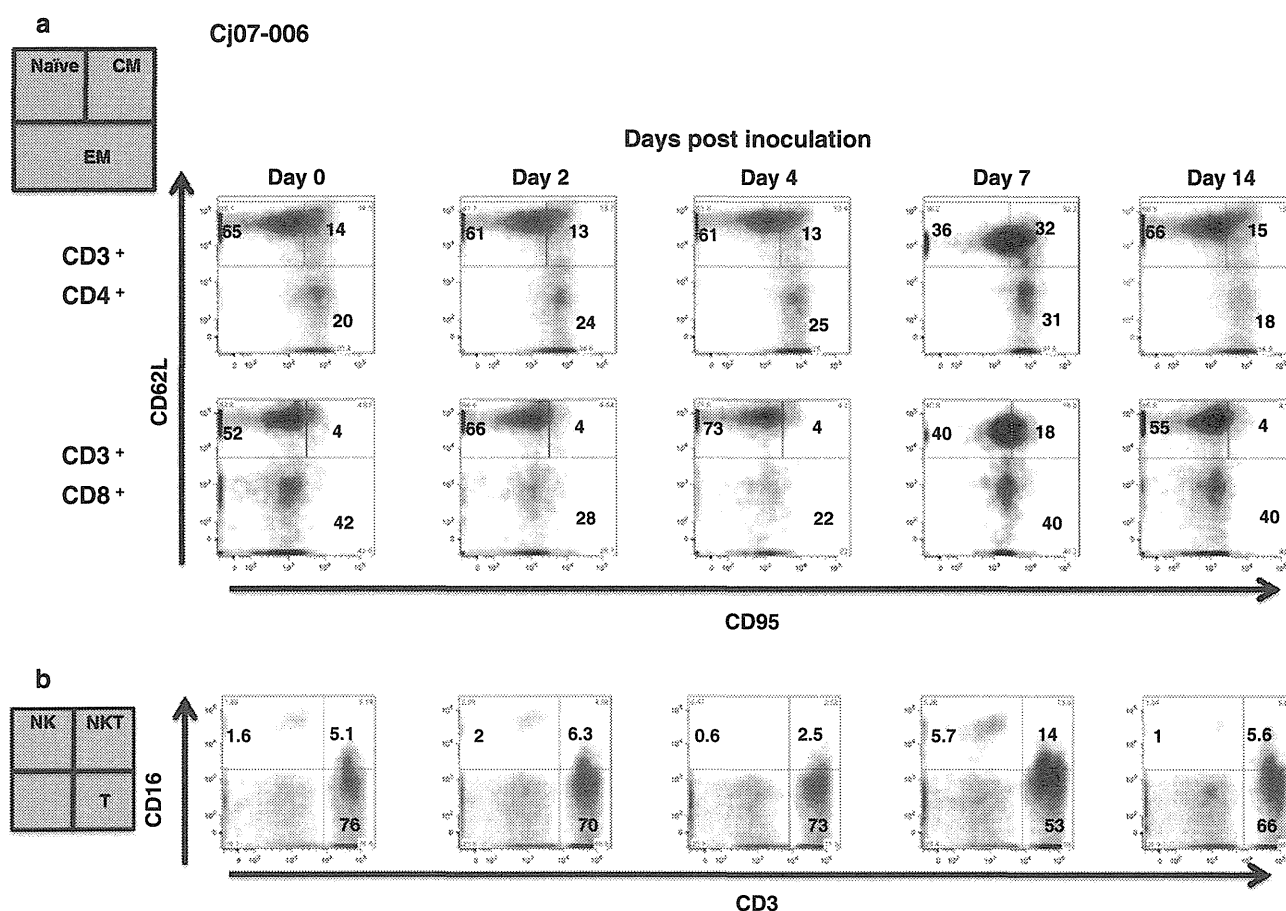


**Fig. 4 Profiling of CD4 and CD8 T, NK and NKT cells in marmosets with primary infection with the DENV-2 DHF0663 strain.** For primary DENV infection, two marmosets were inoculated subcutaneously in the back with  $1.8 \times 10^4$  PFU of the DENV-2

DHF0663 strain. (a) Profiling of naïve, central memory, and effector memory CD4 and CD8 T cells in total CD4 and CD8 T cells. (b) Profiling of NK and NKT cells in total lymphocytes. (a–b) Cj07-006

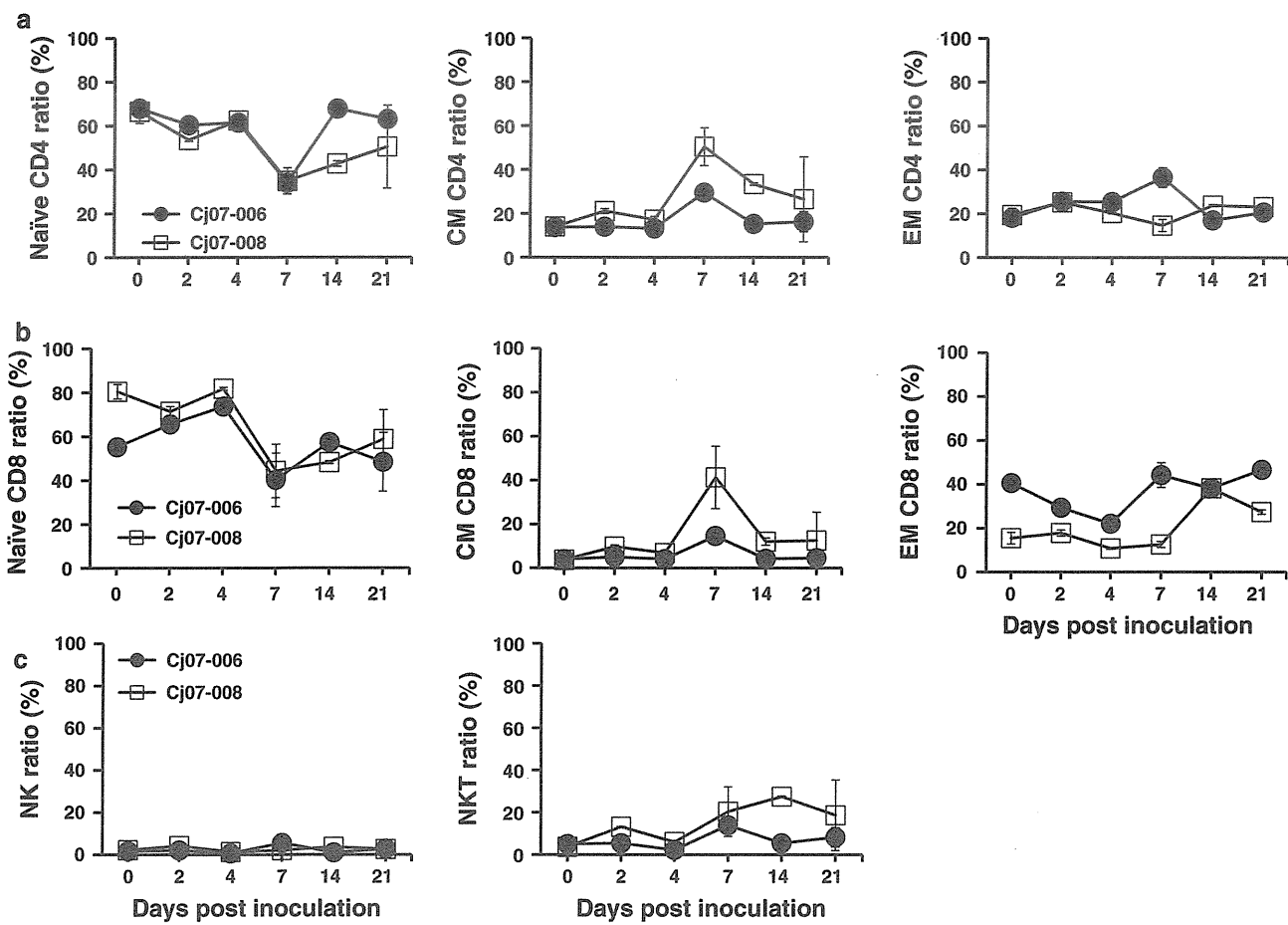


**Fig. 5** Frequency of CD4 and CD8 T, NK and NKT cells in marmosets with primary infection with the DENV-2 DHF0663 strain. For primary DENV infection, two marmosets were inoculated subcutaneously in the back with  $1.8 \times 10^4$  PFU of the DENV-2 DHF0663 strain. (a) Ratios of naïve, central memory, and effector

memory CD4 T cells in total CD4 T cells. (b) Ratios of naïve, central memory, and effector memory CD8 T cells in total CD8 T cells. (c) Ratios of NK and NKT cells in total lymphocytes. (a-c) Cj07-006, Cj07-008

**Table 3** Subpopulation ratios of lymphocytes in marmosets during primary DENV infection (DHF0663)

Subpopulation name		Subpopulation ratios (Mean $\pm$ SD: %)					
		Days after inoculation					
		Day 0	Day 2	Day 4	Day 7	Day 14	Day 21
CD3 <sup>+</sup> CD4 <sup>+</sup> CD62L <sup>+</sup> CD95 <sup>-</sup>	(CD4 T <sub>N</sub> )	67.3 $\pm$ 3.6	57.0 $\pm$ 4.0	61.9 $\pm$ 0.9	34.4 $\pm$ 3.6	55.2 $\pm$ 14	56.7 $\pm$ 13
CD3 <sup>+</sup> CD4 <sup>+</sup> CD62L <sup>+</sup> CD95 <sup>+</sup>	(CD4 T <sub>CM</sub> )	13.9 $\pm$ 1.3	17.5 $\pm$ 4.1	15.2 $\pm$ 2.5	40.0 $\pm$ 13	33.8 $\pm$ 10	21.3 $\pm$ 12
CD3 <sup>+</sup> CD8 <sup>+</sup> CD62L <sup>-</sup> CD95 <sup>±</sup>	(CD4 T <sub>EM</sub> )	18.8 $\pm$ 2.2	25.3 $\pm$ 0.9	22.8 $\pm$ 2.9	25.6 $\pm$ 13	20.3 $\pm$ 4.0	21.8 $\pm$ 1.5
CD3 <sup>+</sup> CD8 <sup>+</sup> CD62L <sup>+</sup> CD95 <sup>-</sup>	(CDS T <sub>N</sub> )	67.8 $\pm$ 14	68.4 $\pm$ 3.7	77.7 $\pm$ 4.6	42.2 $\pm$ 7.4	52.7 $\pm$ 5.5	53.5 $\pm$ 9.8
CD3 <sup>+</sup> CD8 <sup>+</sup> CD62L <sup>+</sup> CD95 <sup>-</sup>	(CDS T <sub>CM</sub> )	3.9 $\pm$ 0.6	7.4 $\pm$ 2.8	5.5 $\pm$ 1.6	28 $\pm$ 17	8.1 $\pm$ 4.6	8.6 $\pm$ 8.9
CD3 <sup>+</sup> CD8 <sup>+</sup> CD62L <sup>-</sup> CD95 <sup>±</sup>	(CDS T <sub>EM</sub> )	28 $\pm$ 14	23.5 $\pm$ 6.7	16.4 $\pm$ 6.5	28.3 $\pm$ 18	38.2 $\pm$ 1.9	37.0 $\pm$ 11
CD3 <sup>-</sup> CD16 <sup>+</sup>	(NK)	4.7 $\pm$ 1.0	4.2 $\pm$ 1.9	2.0 $\pm$ 1.1	6.3 $\pm$ 2.3	5.1 $\pm$ 2.2	7.3 $\pm$ 1.2
CD3 <sup>+</sup> CD16 <sup>+</sup>	(NKT)	7.8 $\pm$ 1.0	9.3 $\pm$ 4.5	5.9 $\pm$ 2.6	22.6 $\pm$ 8.4	20.6 $\pm$ 10	17.3 $\pm$ 10

SD: Standard deviation

Results shown are mean  $\pm$  SD from 2 marmosets as shown in Figure 5

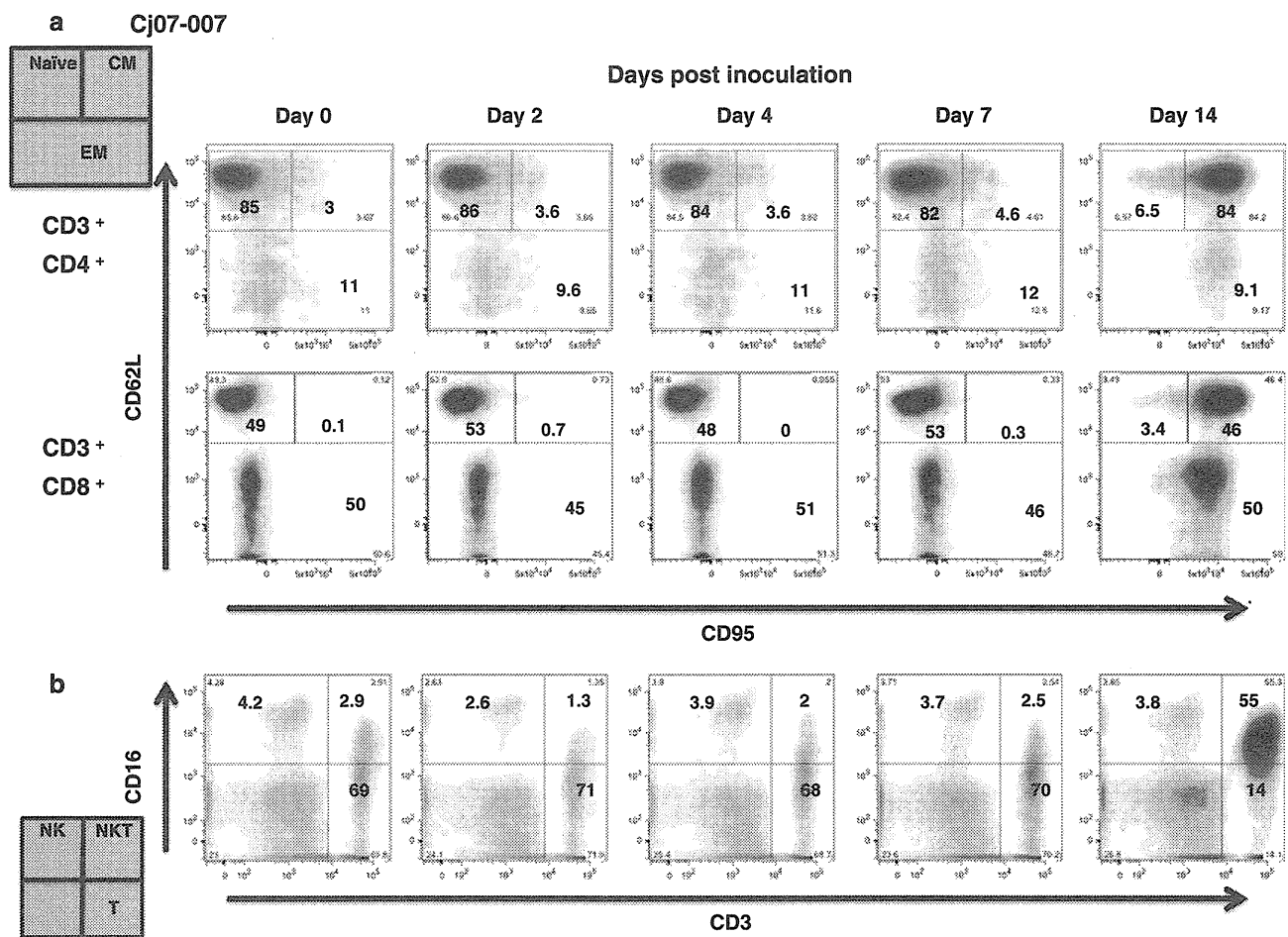


**Fig. 6** Profiling of CD4 and CD8 T, NK and NKT cells in marmosets after re-challenge with the DENV-2 DHF0663 strain. Two marmosets that were initially inoculated with  $1.8 \times 10^5$  PFU of the DHF0663 strain were re-inoculated 33 weeks after the primary

challenge with  $1.8 \times 10^5$  PFU of the same strain. **(a)** Profiling of naive, central memory, and effector memory CD4 and CD8 T cells in total CD4 and CD8 T cells. **(b)** Profiling of NK and NKT cells in total lymphocytes. **(a-b)** Cj07-007

CD4<sup>+</sup> T<sub>N</sub> cells decreased strongly at the same time. CD4<sup>+</sup> T<sub>EM</sub> cells maintained their initial levels through the observation period. Similarly, CD8<sup>+</sup> T<sub>CM</sub> and NKT cells clearly increased on day 14 post-inoculation. Importantly, these T cell responses were induced one week after the obvious induction of the neutralizing antibody in the marmosets [24]. These results suggest that the neutralizing antibody may play a critical role in the complete inhibition of the secondary DENV infection.

## Discussion

In this study, we demonstrated the dynamics of the central/effector memory T cells and NK/NKT subsets against DENV infection in our marmoset model. First, we characterized the central/effector memory T and NK/NKT subsets in marmosets (Fig. 1). Second, we found that CD4/CD8 central memory T cells and NKT cells had significant

responses in the primary DENV infection, and the levels appeared to be dependent on the strain of the virus employed for challenge experiments (Figs. 2–5). Finally, we found delayed responses of CD4/CD8 central memory T cells in the monkeys re-challenged with the same DENV DHF strain, despite the complete inhibition of DENV replication (Figs. 6–7).

The present study shed light on the dynamics of cellular and humoral immune responses against DENV *in vivo* in the marmoset model. Our results showed that cellular immune responses were induced earlier than antibody responses in the primary infection. Thus, our results suggest the possibility that cellular immunity may contribute, at least in part, to the control of primary DENV infection. On the other hand, in the presence of neutralizing antibodies in the re-challenged monkeys [24], delayed (on day 14 after the re-challenge) responses of CD4/CD8 central memory T cells were observed despite the complete inhibition of DENV replication. These results indicate that

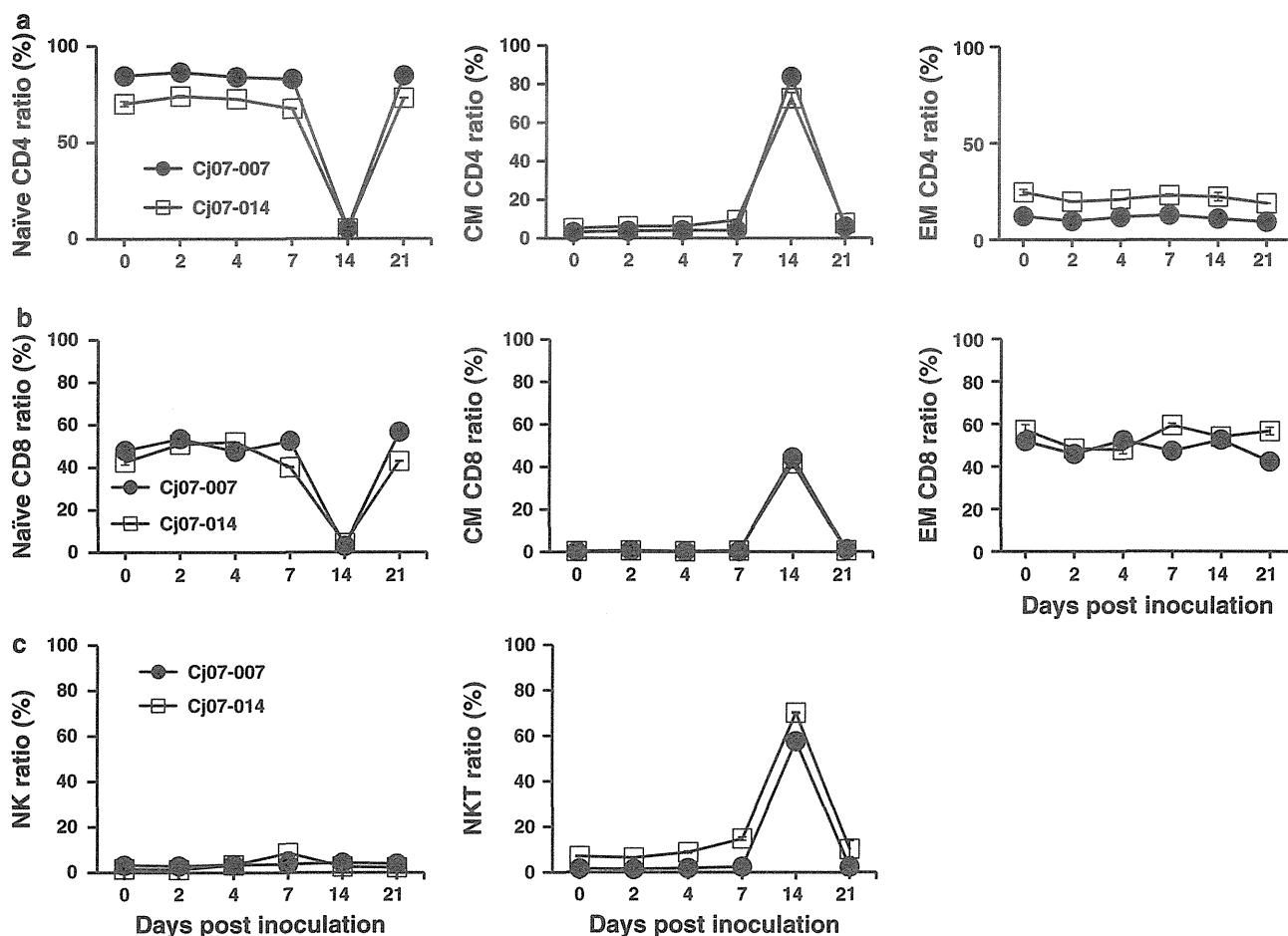


**Fig. 7** Frequency of CD4 and CD8 T, NK and NKT cells in marmosets after re-challenge with the DENV-2 DHF0663 strain. Two marmosets initially inoculated with  $1.8 \times 10^5$  PFU of the DHF0663 strain were re-inoculated 33 weeks after the primary challenge with  $1.8 \times 10^5$  PFU of the same strain. (a) Ratios of naïve,

central memory, and effector memory CD4 T cells in total CD4 T cells. (b) Ratios of naïve, central memory, and effector memory CD8 T cells in total CD8 T cells. (c) Ratios of NK and NKT cells in total lymphocytes. (a-c) Cj07-007, Cj07-014

cellular immunity is unlikely to play a major role in the control of DENV re-infection. Alternatively, it is still possible that components of cellular immunity, such as memory T cells, could partially play a helper role for the enhanced induction of neutralizing antibodies even without an apparent increase in the proportion of  $T_{CM}$ , resulting in efficient prevention of DENV replication.

It is possible that the DENV strains used in this study influence the strength of cellular immune responses. The differences in cellular immune responses between the monkeys infected with the DF and DHF strains are probably not caused by individual differences in the marmosets, because the FACS results were consistent with each pair of marmosets. It was shown previously that there was a reduction in CD3, CD4, and CD8 cells in DHF and that lower levels of CD3, CD4, and CD8 cells discriminated DHF from DF patients during the febrile stage of illness [5]. There was a significant increase in an early activation

marker on  $CD8^+$  T cells in children with DHF compared with DF during the febrile period of illness [8]. Another group reported that levels of peripheral blood mononuclear cell apoptosis were higher in children developing DHF [23]. Moreover, cDNA array and ELISA screening demonstrated that IFN-inducible genes, IFN-induced genes and IFN production were strongly up-regulated in DF patients when compared to DHF patients, suggesting a significant role of the IFN system during infection with DF strains when compared to DHF strains [34]. Thus, it is reasonable to assume that DHF strains might have the ability to negatively regulate T cell responses. A recent report demonstrating that the sequence of a DHF strain differed from that of a DF strain at six unique amino acid residues located in the membrane, envelope and non-structural genes [33], which supports our notion.

Alternatively, another possibility is that the strength of T cell responses might depend on the viral load. In fact, in

our results, the stronger T cell responses in monkeys infected with the DF strain were paralleled by higher viral loads, which was in contrast to the result obtained with DHF-strain-infected animals with lower viral loads. Of note, the tenfold higher challenge dose of the DF strain used in this study ( $1.9 \times 10^5$  PFU) compared to the DHF strain ( $1.8 \times 10^4$  PFU) could have simply led to tenfold higher peak viral RNA levels in monkeys infected with the DF strain. In either case, the relationship between the strength of the antiviral immune response and the viral strain remains to be elucidated. Further *in vivo* characterization of the antiviral immunity and the viral replication kinetics induced by infection with various DENV strains isolated from DF and DHF patients will help to understand the mechanism of differential disease progression in the course of DENV infection.

We observed that dengue vRNA was not detected in plasma samples from marmosets re-infected with the same DENV-2 DHF strain 33 weeks after the primary infection. This result suggests that memory B cells induced in the primary DENV infection were predominantly activated to produce neutralizing antibodies against the same DHF strain in the secondary infection in the absence of apparent cellular immune responses. A previous report showed that DENV infection induces a high-titered neutralizing antibody that can provide long-term immunity to the homologous DENV serotype [22], which is consistent with our results. By contrast, the role of cellular immune responses in the control of DENV infection remains to be elucidated. Our results in this study may suggest that cellular immune responses and neutralizing antibodies acted cooperatively to control primary DENV infection. In DENV-infected patients, it may be difficult to distinguish whether each case is primary or secondary DENV infection and also to serially collect blood samples for immunological study in the course of the infection, which is likely to be the reason for the discrepancy regarding the importance of cellular immunity in DENV infection. From this point of view, our marmoset model of DENV infection will further provide important information regarding the role of cellular immune responses in DENV infection.

**Acknowledgments** We would like to give special thanks to members of The Corporation for Production and Research of Laboratory Primates for technical assistance. We also appreciate Ms. Tomoko Ikoma and Mizuho Fujita for technical assistance. This work was supported by grants from the Ministry of Health, Labor and Welfare of Japan, and by the Environment Research and Technology Development Fund (D-1007) from the Ministry of the Environment of Japan.

**Conflict of interest** The authors declare that the research was conducted in the absence of any commercial or financial relationships that could be construed as a potential conflict of interest.

## References

1. Balsitis SJ, Williams KL, Lachica R, Flores D, Kyle JL, Mehlhop E, Johnson S, Diamond MS, Beatty PR, Harris E (2010) Lethal antibody enhancement of dengue disease in mice is prevented by Fc modification. *PLoS Pathog* 6:e1000790
2. Beaumier CM, Mathew A, Bashyam HS, Rothman AL (2008) Cross-reactive memory CD8(+) T cells alter the immune response to heterologous secondary dengue virus infections in mice in a sequence-specific manner. *J Infect Dis* 197:608–617
3. Beaumier CM, Rothman AL (2009) Cross-reactive memory CD4+ T cells alter the CD8+ T-cell response to heterologous secondary dengue virus infections in mice in a sequence-specific manner. *Viral Immunol* 22:215–219
4. Beaumier CM, Jaiswal S, West KY, Friberg H, Mathew A, Rothman AL (2010) Differential *in vivo* clearance and response to secondary heterologous infections by H2(b)-restricted dengue virus-specific CD8+ T cells. *Viral Immunol* 23:477–485
5. Fadilah SA, Sahrir S, Raymond AA, Cheong SK, Aziz JA, Sivagengei K (1999) Quantitation of T lymphocyte subsets helps to distinguish dengue hemorrhagic fever from classic dengue fever during the acute febrile stage. *Southeast Asian J Trop Med Public Health* 30:710–717
6. Goncalves AP, Engle RE, St Claire M, Purcell RH, Lai CJ (2007) Monoclonal antibody-mediated enhancement of dengue virus infection *in vitro* and *in vivo* and strategies for prevention. *Proc Natl Acad Sci USA* 104:9422–9427
7. Green S, Pichyangkul S, Vaughn DW, Kalayanarooj S, Nimmannitya S, Nisalak A, Kurane I, Rothman AL, Ennis FA (1999) Early CD69 expression on peripheral blood lymphocytes from children with dengue hemorrhagic fever. *J Infect Dis* 180:1429–1435
8. Green S, Vaughn DW, Kalayanarooj S, Nimmannitya S, Suntayakorn S, Nisalak A, Lew R, Innis BL, Kurane I, Rothman AL, Ennis FA (1999) Early immune activation in acute dengue illness is related to development of plasma leakage and disease severity. *J Infect Dis* 179:755–762
9. Gupta S, Gollapudi S (2008) CD95-mediated apoptosis in naive, central and effector memory subsets of CD4+ and CD8+ T cells in aged humans. *Exp Gerontol* 43:266–274
10. Guzman MG, Alvarez M, Rodriguez-Roche R, Bernardo L, Montes T, Vazquez S, Morier L, Alvarez A, Gould EA, Kouri G, Halstead SB (2007) Neutralizing antibodies after infection with dengue 1 virus. *Emerg Infect Dis* 13:282–286
11. Halstead SB (1979) *In vivo* enhancement of dengue virus infection in rhesus monkeys by passively transferred antibody. *J Infect Dis* 140:527–533
12. Halstead SB (2007) Dengue. *Lancet* 370:1644–1652
13. Henchal EA, Henchal LS, Schlesinger JJ (1988) Synergistic interactions of anti-NS1 monoclonal antibodies protect passively immunized mice from lethal challenge with dengue 2 virus. *J Gen Virol* 69(Pt 8):2101–2107
14. Hus I, Staroslawska E, Bojarska-Junak A, Dobrzynska-Rutkowska A, Surdacka A, Wdowiak P, Wasiak M, Kusz M, Twardosz A, Dmoszynska A, Rolinski J (2011) CD3+/CD16+CD56+ cell numbers in peripheral blood are correlated with higher tumor burden in patients with diffuse large B-cell lymphoma. *Folia Histochem Cytobiol* 49:183–187
15. Kaufman BM, Summers PL, Dubois DR, Eckels KH (1987) Monoclonal antibodies against dengue 2 virus E-glycoprotein protect mice against lethal dengue infection. *Am J Trop Med Hyg* 36:427–434
16. Kaufman BM, Summers PL, Dubois DR, Cohen WH, Gentry MK, Timchak RL, Burke DS, Eckels KH (1989) Monoclonal

- antibodies for dengue virus prM glycoprotein protect mice against lethal dengue infection. *Am J Trop Med Hyg* 41:576–580
17. Khvedelidze M, Chkhartishvili N, Abashidze L, Dzigua L, Tsertsvadze T (2008) Expansion of CD3/CD16/CD56 positive NKT cells in HIV/AIDS: the pilot study. *Georgian Med News* 165:78–83
  18. Kyle JL, Balsitis SJ, Zhang L, Beatty PR, Harris E (2008) Antibodies play a greater role than immune cells in heterologous protection against secondary dengue virus infection in a mouse model. *Virology* 380:296–303
  19. Mathew A, Rothman AL (2008) Understanding the contribution of cellular immunity to dengue disease pathogenesis. *Immunol Rev* 225:300–313
  20. Mladinich KM, Piaskowski SM, Rudersdorf R, Eernisse CM, Weisgrau KL, Martins MA, Furlott JR, Partidos CD, Brewoo JN, Osorio JE, Wilson NA, Rakasz EG, Watkins DI (2012) Dengue virus-specific CD4+ and CD8+ T lymphocytes target NS1, NS3 and NS5 in infected Indian rhesus macaques. *Immunogenetics* 64:111–121
  21. Mueller YM, Makar V, Bojczuk PM, Witek J, Katsikis PD (2003) IL-15 enhances the function and inhibits CD95/Fas-induced apoptosis of human CD4+ and CD8+ effector-memory T cells. *Int Immunol* 15:49–58
  22. Murphy BR, Whitehead SS (2011) Immune response to dengue virus and prospects for a vaccine. *Annu Rev Immunol* 29:587–619
  23. Myint KS, Endy TP, Mongkolsirichaikul D, Manomuth C, Kalayanaroj S, Vaughn DW, Nisalak A, Green S, Rothman AL, Ennis FA, Libraty DH (2006) Cellular immune activation in children with acute dengue virus infections is modulated by apoptosis. *J Infect Dis* 194:600–607
  24. Omatsu T, Moi ML, Hirayama T, Takasaki T, Nakamura S, Tajima S, Ito M, Yoshida T, Saito A, Katakai Y, Akari H, Kurane I (2011) Common marmoset (*Callithrix jacchus*) as a primate model of dengue virus infection: development of high levels of viremia and demonstration of protective immunity. *J Gen Virol* 92:2272–2280
  25. Omatsu T, Moi ML, Takasaki T, Nakamura S, Katakai Y, Tajima S, Ito M, Yoshida T, Saito A, Akari H, Kurane I (2013) Changes in hematological and serum biochemical parameters in common marmosets (*Callithrix jacchus*) after inoculation with dengue virus. *J Med Primatol* 54:89–98
  26. Onlamoon N, Noisakran S, Hsiao HM, Duncan A, Villinger F, Ansari AA, Perng GC (2010) Dengue virus-induced hemorrhage in a nonhuman primate model. *Blood* 115:1823–1834
  27. Pawitan JA (2011) Dengue virus infection: predictors for severe dengue. *Acta Med Indones* 43:129–135
  28. Pitcher CJ, Hagen SI, Walker JM, Lum R, Mitchell BL, Maino VC, Axthelm MK, Picker LJ (2002) Development and homeostasis of T cell memory in rhesus macaque. *J Immunol* 168:29–43
  29. Rigau-Perez JG, Clark GG, Gubler DJ, Reiter P, Sanders EJ, Vorndam AV (1998) Dengue and dengue haemorrhagic fever. *Lancet* 352:971–977
  30. Sabin AB (1950) The dengue group of viruses and its family relationships. *Bacteriol Rev* 14:225–232
  31. Sierra B, Garcia G, Perez AB, Morier L, Rodriguez R, Alvarez M, Guzman MG (2002) Long-term memory cellular immune response to dengue virus after a natural primary infection. *Int J Infect Dis* 6:125–128
  32. Terabe M, Berzofsky JA (2008) The role of NKT cells in tumor immunity. *Adv Cancer Res* 101:277–348
  33. Tuiskunen A, Monteil V, Plumet S, Boubis L, Wahlstrom M, Duong V, Buchy P, Lundkvist A, Tolou H, Leparc-Goffart I (2011) Phenotypic and genotypic characterization of dengue virus isolates differentiates dengue fever and dengue hemorrhagic fever from dengue shock syndrome. *Arch Virol* 156:2023–2032
  34. Ubol S, Masrinoul P, Chaijaruwanich J, Kalayanaroj S, Charoensirisuthikul T, Kasisith J (2008) Differences in global gene expression in peripheral blood mononuclear cells indicate a significant role of the innate responses in progression of dengue fever but not dengue hemorrhagic fever. *J Infect Dis* 197:1459–1467
  35. Yauch LE, Zellweger RM, Kotturi MF, Qutubuddin A, Sidney J, Peters B, Prestwood TR, Sette A, Shresta S (2009) A protective role for dengue virus-specific CD8+ T cells. *J Immunol* 182:4865–4873
  36. Yauch LE, Prestwood TR, May MM, Morar MM, Zellweger RM, Peters B, Sette A, Shresta S (2010) CD4+ T cells are not required for the induction of dengue virus-specific CD8+ T cell or antibody responses but contribute to protection after vaccination. *J Immunol* 185:5405–5416
  37. Yoshida T, Saito A, Iwasaki Y, Iijima S, Kurosawa T, Katakai Y, Yasutomi Y, Reimann KA, Hayakawa T, Akari H (2010) Characterization of natural killer cells in tamarins: a technical basis for studies of innate immunity. *Front Microbiol* 1:128
  38. Yoshida T, Omatsu T, Saito A, Katakai Y, Iwasaki Y, Iijima S, Kurosawa T, Hamano M, Nakamura S, Takasaki T, Yasutomi Y, Kurane I, Akari H (2012) CD16(+) natural killer cells play a limited role against primary dengue virus infection in tamarins. *Arch Virol* 157:363–368
  39. Zompi S, Santich BH, Beatty PR, Harris E (2012) Protection from secondary dengue virus infection in a mouse model reveals the role of serotype cross-reactive B and T cells. *J Immunol* 188:404–416

# Novel Role of HSP40/DNAJ in the Regulation of HIV-1 Replication

Emiko Urano, PhD,\* Yuko Morikawa, DVM, PhD,† and Jun Komano, MD, PhD\*‡

**Objectives:** DNAJ/HSP40 is an evolutionarily conserved family of proteins bearing various functions. Historically, it has been emphasized that HSP40/DNAJ family proteins play a positive role in infection of various viruses. We identified DNAJ/HSP40B6 as a potential negative regulator of HIV-1 replication in our genetic screens. In this study, we investigated the functional interactions between HIV-1 and HSP40 family members.

**Design:** We took genetic and comparative virology approaches to expand the primary observation.

**Methods:** Multiple HSP40/DNAJ proteins were tested for their ability to inhibit replication of adenovirus, herpes simplex virus type 1, HIV-1, and vaccinia virus. The mechanism of inhibition was investigated by using HSP40/DNAJ mutants and measuring the efficiencies of each viral replication steps.

**Results:** HSP40A1, B1, B6, and C5, but not C3, were found to be able to limit HIV-1 production. This effect was specific to HIV-1 for such effects were not detected in adenovirus, herpes simplex virus type 1, and vaccinia virus. Genetic analyses suggested that the conserved DNAJ domain was responsible for the inhibition of HIV-1 production through which HSP40 regulates HSP70 ATPase activity. Interestingly, HSP40s lowered the levels of steady-state viral messenger RNA. This was not attributed to the inhibition of Tat/long terminal repeat-driven transcription but the downregulation of Rev expression.

**Conclusions:** This is the first report providing evidence that HSP70-HSP40 complex confers an innate resistance specific to HIV-1. For their interferon-inducible nature, HSP40 family members should account for the anti-HIV-1 function of interferon.

**Key Words:** HSP40, DNAJ, HIV-1 replication, HSP70-HSP40 axis, viral RNA accumulation, interferon-alpha

(*J Acquir Immune Defic Syndr* 2013;64:154–162)

## INTRODUCTION

DNAJ/HSP40 is an evolutionarily conserved family of proteins that perform functions including regulation of transcription, translation, and protein folding.<sup>1–4</sup> The human genome encodes more than 40 identified HSP40 family members, which can be classified into 3 groups (A, B, and C) according to their domain structures.<sup>1–3</sup> In eukaryotic cells, HSP40 physically interacts with HSP70 through the DNAJ domain and activates the ATPase activity associated with HSP70. HSP70 supports protein folding and is therefore a chaperone; HSP40 regulates HSP70 and is thus a cochaperone. Many HSP40 family proteins are expressed constitutively in a variety of tissues.<sup>1–3</sup> However, not all human HSP40 proteins are well characterized.

Distinct HSP40 family members regulate replication and pathogenesis of various viruses.<sup>5</sup> Among viruses that infect humans, HSP40 subfamily A member 1 (A1)/Hdj2 regulates replication of Japanese encephalitis virus<sup>6</sup>; HSP40A3, hepatitis B virus, and human T-cell leukemia virus type 1<sup>7,8</sup>; HSP40B1/hTid-1, adenovirus (AdV),<sup>9</sup> herpes simplex virus type 1 (HSV-1),<sup>10</sup> and HIV-1<sup>11,12</sup>; HSP40B6/Hdj1 and HIV-2<sup>13</sup>; HSP40B11/ERdj3, B12, B14, and C18 regulate simian virus 40 (SV40)<sup>14</sup>; HSP40C3/IPK58/P58<sup>IPK</sup> and influenza virus (IFV)<sup>15</sup>; and HSP40J14 and flavivirus.<sup>16</sup> The mechanisms of action vary among HSP40s and viruses. HSP40C3 is one of the most well-studied HSP40 proteins. IFV infection activates HSP40C3, a negative regulator of interferon-induced RNA-activated protein kinase (PKR). HSP40C3 along with HSP70 binds to PKR, thereby promoting efficient translation of viral messenger RNA (mRNA) in IFV-infected cells.<sup>15</sup> Before now, it has not been clear to what extent cochaperone activity is involved in the PKR–P58<sup>IPK</sup> interaction. The importance of the DNAJ domain is also suggested by the fact that simian virus 40 large T antigen contains a DNAJ domain required for viral replication and cell transformation.<sup>17</sup> These studies identified HSP40 as a positive regulator of viral replication. By contrast, it has been reported that HSP40A3 and HSP40B6/Hdj1 negatively regulate hepatitis B virus replication.<sup>7</sup>

We have established a functional complementary DNA (cDNA) library screen for isolating genes that regulate HIV-1 using replication-competent virus.<sup>18–20</sup> We performed 2 genetic screens, one in a human CD4<sup>+</sup> T-cell line, MT-4, and other in a genetically modified HeLa cell line, TZM-bl. In the former screen, the cDNA-encoding HSP40B6 was isolated at

Received for publication December 21, 2012; accepted May 1, 2013.

From the \*AIDS Research Center, National Institute of Infectious Diseases, Tokyo, Japan; †Kitasato Institute for Life Sciences, Graduate School of Infection Control, Kitasato University, Tokyo, Japan; and ‡Department of Infectious Diseases, Virology Division, Osaka Prefectural Institute of Public Health, Osaka, Japan (Dr Urano is now with the Virus-Cell Interaction Section, HIV Drug Resistance Program, National Cancer Institute, Frederick, MD).

Supported by the Japan Health Science Foundation; the Japanese Ministry of Health, Labor, and Welfare and the Japanese Ministry of Education, Culture, Sports, Science and Technology.

E.U., Y.M., and J.K. designed and performed the experiments and interpreted the data. J.K. and E.U. wrote the manuscript.

The authors have no conflicts of interest to disclose.

Correspondence to: Jun Komano, MD, PhD, Osaka Prefectural Institute of Public Health, Department of Infectious Diseases, Virology Division, 3-69, Nakamachi, 1-chome, Higashinari-ku, Osaka 537-0025, Japan (e-mail: komano@iph.pref.osaka.jp).

Copyright © 2013 by Lippincott Williams & Wilkins

a frequency of 14.3% (6/42 clones) from a cDNA library prepared from the rabbit epithelial cell line RK13. In the latter screen, the same gene was isolated at a frequency of 32.0% (8/25 clones) from a cDNA library prepared from MT-4 cells. In our genetic screens, HSP40B6 was scored as a negative regulator of HIV-1 replication. An additional screen using a small interfering RNA (siRNA) mini-library<sup>21</sup> demonstrated that the downregulation of HSP40B6 slightly enhanced the production of HIV-1. These data strongly suggest that HSP40B6 is expressed constitutively in T cells and negatively regulates HIV-1 replication by targeting the production phase of the viral life cycle. In this study, we investigated the functional interactions between HIV-1 and HSP40 family members.

## METHODS

### Cells and Transfection

All mammalian cells were maintained in RPMI 1640 (Sigma, St Louis, MO) supplemented with 10% fetal bovine serum (FBS) (Japan Bioserum, Tokyo, Japan), penicillin, and streptomycin (Invitrogen, Tokyo, Japan). Cells were incubated at 37°C in a humidified 5% of CO<sub>2</sub> atmosphere. Cells were transfected using Lipofectamine 2000 (Invitrogen).

### Plasmids and RNA Interference

Expression vectors for HSP40 mutants and mCherry tagged with HA epitope were generated by standard molecular cloning technology under the background of pCMMP,<sup>22</sup> pcDNA3 (Invitrogen), and pEGFP (Clontech, Palo Alto, CA) vectors. The HA-tagged Rev expression vector based on pcDNA3 (Invitrogen) was produced based on the HIV-1<sub>SF2</sub> Rev. The following plasmids were described previously: psynag-pol,<sup>23</sup> pCMV8.91,<sup>24</sup> pSV-Tat.<sup>22</sup> The nucleic acid sequences for RNA interference with HSP40A1, B6, and CCR5 expression are as follows: A1 sense and antisense strands, 5'-GAU CAG UCC UAA AGA UAG AdTdT-3' and 5'-UCU AUC UUU AGG ACU GAU CdTdT-3'; B6 sense and antisense strands, 5'-GGG CAA CUU CAA AUC GAU AdTdT-3' and 5'-UAU CGA UUU GAA GUU GCC CdTdT-3' (B-Bridge International, Inc, Tokyo, Japan); and CCR5 sense and antisense strands, 5'-CUU UUG ACA GGG CUC UAU UUU-3' and 5'-AAU AGA GCC CUG UCA AGA GUU-3' (RNAi, Inc, Tokyo, Japan).

### Reporter Assay

Luciferase and beta-galactosidase activities were measured 48–72 hours after transfection or infection using the DualGlo assay kit (Promega, Madison, WI) or the LumiGal assay kit (Clontech).

### Generating Viruses

To produce HIV-1, 293T cells were transfected with plasmids encoding HIV-1<sub>HXB2</sub> proviral DNA, and culture supernatants were collected 48 hours posttransfection. Murine leukemia virus (MLV) and HIV-1–based lentiviral vectors

pseudotyped with VSV-G were produced as described previously.<sup>22,25</sup> The preparations of vaccinia virus (VV; intracellular mature virus), HSV-1, and adenoviral vectors were described previously.<sup>22</sup>

### Measuring Viral Production and Replication

To monitor HIV-1 production and replication, p24<sup>CA</sup> antigen was detected using the Retro TEK p24 antigen ELISA kit (Zepto Metrix, Buffalo, NY). For VV, AdV, and HSV-1, viral replication was assessed by measuring reporter gene activities as previously described.<sup>22</sup>

### Western Blotting and Immunoprecipitation

Western blotting and immunoprecipitation were performed according to previously described techniques.<sup>26,27</sup> The following reagents were used: anti-FLAG (F7425; Sigma), anti-HA polyclonal antibody (Sigma), anti-p24<sup>CA</sup> (CA, 183-H12-5C, NIH AIDS Research and Reference Reagent Program), anti-actin (clone MAB1501R; Millipore, Tokyo, Japan), anti-BiP/GRP78 (clone 40; Clontech), biotinylated antigoat antibodies (GE Healthcare, Tokyo, Japan), streptavidin-HRP (GE Healthcare), and Envision<sup>+</sup> Dual Link System-HRP (Dako, Glostrup, Denmark).

### Immunofluorescence Assay

Intracellular distributions of HSP40 proteins were analyzed by immunofluorescence microscopy of transfected 293T cells as described previously.<sup>28</sup>

### Reverse Transcriptase–Polymerase Chain Reaction

Total RNA isolation and reverse transcriptase-polymerase chain reaction assays were performed as described previously.<sup>18</sup> Amplicons were electrophoresed in agarose gels, stained with ethidium bromide, imaged with a Typhoon 9400 scanner (GE Healthcare), and quantified with ImageQuant software (GE Healthcare). For the amplification of HIV-1 Vpr and glyceraldehyde-3-phosphate dehydrogenase cDNAs, primers were as described previously.<sup>18,27</sup>

## RESULTS

### Restriction of HIV-1 Production by Diverse HSP40 Proteins

We first investigated whether any HSP40 family members are able to inhibit HIV-1 production. HSP40A1, B1, B6, C3, and C5 were chosen because they are evolutionarily distant from one another and have reported to be involved in viral pathogenesis (Fig. 1A). Each gene was cloned into mammalian expression vectors under control of the cytomegalovirus (CMV) promoter and tagged with a FLAG epitope at the 5' end. The expression of each HSP40 was verified by Western blot analysis (Fig. 1B). Two bands were detected for HSP40C5, probably due to the posttranslational modification. The levels of HSP40C3 expression were not as high as those of other

members. All HSP40 proteins were distributed mainly in the cytoplasm (Fig. 1C). HSP40A1 exhibited a homogenous cytoplasmic distribution. HSP40B6 and C5 exhibited homogenous cytoplasmic distributions with fine speckles, whereas B1 and C3 accumulated in slightly larger cytoplasmic speckles. In transient transfection assays in which the HIV-1 proviral DNA was co-transfected into 293T cells along with HSP40 expression vectors, the production levels of HIV-1 were significantly attenuated by HSP40A1, B1, B6, and C5 to  $22.9\% \pm 14.9\%$ ,  $25.5\% \pm 26.0\%$ ,  $33.8\% \pm 15.1\%$ , and  $11.3\% \pm 11.1\%$ , respectively, as measured by the level of viral p24 capsid antigen (p24<sup>CA</sup>) in the culture supernatant ( $P < 0.001$  by 2-sided Student *t* test; Fig. 1D). HSP40C3 was unable to limit HIV-1 production ( $86.4\% \pm 30.5\%$ ,  $P = 0.30$  by 2-sided Student *t* test). In agreement with these findings, immunoblot analyses indicated that p24<sup>CA</sup> expression in the virus-producing cells was also attenuated by HSP40A1, B1, B6, and C5, but not by C3 (Fig. 1B, bottom panel). The levels of HSP40C3 were higher than those of some of the B6 mutants that retained the ability to inhibit HIV-1 production (shown below), indicating that the inability of HSP40C3 to limit HIV-1 production was not merely due to low levels of expression; it seems more likely that HSP40C3 lacks the ability to inhibit HIV-1 production.

We next investigated viral specificity by examining the effect of HSP40 expression on the replication of other viruses, including AdV, HSV-1, and VV. The replication efficiencies of AdV were enhanced by HSP40A1 in agreement with a previous report.<sup>9</sup> By contrast, the replication efficiencies of AdV and VV were significantly inhibited by HSP40C5, by 44.7% and 54.8%, respectively ( $P < 0.001$  by 2-sided Student *t* test; Fig. 1E). HSP40B1 slightly reduced the replication of VV, by 24.5% ( $P < 0.001$ ). By contrast, the replication of HSV-1 was not affected by any HSP40 protein (Fig. 1E). Overall, HSP40 family members had different antiviral effects. Control experiments under similar conditions revealed that HSP40 did not affect the expression of beta-galactosidase (Fig. 1E) or firefly luciferase (data not shown) driven by CMV promoters. Thus, inhibition of viral production by HSP40 was specific to HIV-1 and was unlikely due to nonspecific effects.

### Mapping the HSP40 Domain Responsible for the Inhibition of HIV-1 Production

We produced series of mutants for the purpose of identifying the domain of HSP40 proteins that is required for inhibition of HIV-1 production. HSP40A1 and B6 were chosen because B6 was originally isolated in genetic screens, and the constitutive expression of both A1 and B6 was tolerated in human T-cell lines (described below). Furthermore, both A1 and B6 are expressed in T cells.<sup>29–32</sup> We constructed deletion mutants of HSP40A1 and B6 lacking sequences of various lengths from the C-termini and mutants lacking DNAJ domains ( $\Delta$ JD mutants; Figs. 2A, B). Western blotting confirmed that the A1 mutants were expressed efficiently (Fig. 2C), whereas most of the B6 mutants poorly (Fig. 2D), in 293T cells. Cotransfection assays revealed that the A1<sub>1–83</sub> mutant, which contains the DNAJ domain but lacks the C-terminal substrate-binding domain, was more potent than wild-type HSP40s in limiting HIV-1 production (Fig. 2E). By contrast, a mutant lacking the

DNAJ domain was unable to inhibit HIV-1 production (Fig. 2E). Although the levels of expression were low, B6 mutants containing the DNAJ domain were also able to limit HIV-1 production (Fig. 2F). Consistent with the results for A1<sub>1–83</sub>, B6<sub>1–97</sub>, and B6<sub>1–61</sub> mutants lacking most of the C-terminal portion were more potent in inhibiting HIV-1 production than their wild-type counterparts. One exception was the B6<sub>1–121</sub> mutant, which contains the DNAJ domain but failed to limit HIV-1 production (Fig. 2F), possibly because the B6<sub>1–121</sub> protein does not fold properly. The B6 $\Delta$ JD mutant, which lacks the entire DNAJ domain, lost the ability to inhibit HIV-1 production similar to the A1 $\Delta$ JD mutant (Figs. 2E, F). Indeed, HSP40B6 $\Delta$ JD enhanced HIV-1 production by 3.6-fold (Fig. 2F). These data indicate that the DNAJ domain is responsible for the inhibition of HIV-1 production.

HSP40 binds to HSP70 and regulates its ATPase activity. The ATPase regulatory function resides in the DNAJ domain, and the HPD motif at the loop between helices II and III is critical for this function.<sup>1,33</sup> An H-to-Q amino acid substitution in this motif disrupts HSP40's regulation of HSP70 without affecting the HSP70–HSP40 interaction.<sup>1</sup> We produced a mutant containing this substitution, HSP40B6<sub>QPD</sub> (Fig. 2B), and asked whether this mutant could inhibit HIV-1 production. The HSP40B6<sub>QPD</sub> mutant was expressed at levels similar to those of the wild-type protein (Fig. 2D). Levels of HIV-1 production were not affected by HSP40B6<sub>QPD</sub> (Fig. 2F), suggesting that the functional interaction between HSP40 and HSP70, rather than the binding per se, is critical for inhibition of HIV-1 production. These data imply that HSP40 mutants containing the DNAJ domain retain the ability to regulate HSP70's ATPase activity.

To confirm the findings described above, we reduced the expression of HSP40A1 and B6 by RNA interference. The levels of HSP40A1 and B6 proteins produced from the expression vectors were reduced by the cotransfection of corresponding siRNAs (Figs. 2C, D). Cotransfection of siRNAs against HSP40A1 and B6 suppressed the inhibitory effect of these HSP40s on HIV-1 production (Figs. 2E, F). Such effects were not observed in A1<sub>1–83</sub> or B6<sub>1–61</sub>, which lack the siRNA target sequences (Figs. 2E, F). In a similar experimental setting in 293T cells, transfection of siRNA against HSP40A1 or B6 enhanced the levels of HIV-1 production by  $1.4 \pm 0.3$ - or  $1.4 \pm 0.3$ -fold, respectively (5 independent experiments,  $P < 0.05$  by 2-sided Student *t* test). Taken together, these data suggest that the endogenous HSP40 has some abilities to limit HIV-1 production and the inhibition of HIV-1 production could be attributed to the dysregulation of HSP70 functions.

### Impact of HSP40 Expression on the Replication of HIV-1 in T Cells

Next, we examined the impact of HSP40A1 and B6 on HIV-1 replication in T cells. To do this, we introduced HSP40A1 and B6 genes into MT-4 cells using MLV vector, thereby establishing MT-4 cells ectopically expressing HSP40A1 and B6 (Fig. 3A). Constitutive expression of FLAG-tagged HSP40A1 and B6 did not affect the rate of cell proliferation nor the cell-surface levels of CD4 and CXCR4. HIV-1 replication was potently inhibited in MT-4 cells expressing either HSP40A1 or

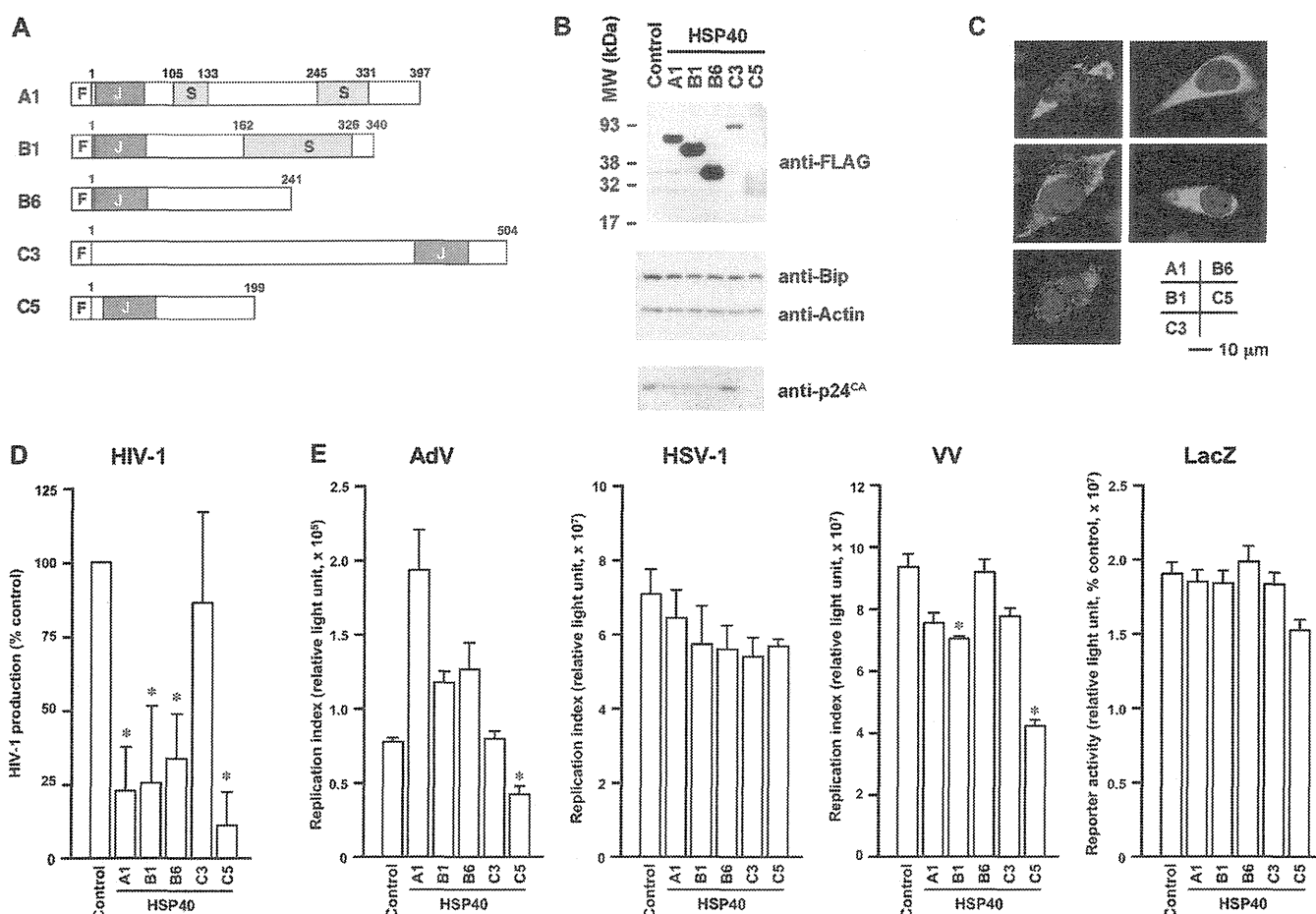


**FIGURE 1.** Inhibition of HIV-1 production by HSP40 family members. A, Domain organization of HSP40A1, B1, B6, C3, and C5. Numbers represent amino acids. DNAJ and the C-terminal substrate-binding domains are shown as J and S, respectively. All HSP40 proteins are tagged with the FLAG epitope at their N-termini, indicated by F. B, Verification of expression of cloned HSP40 proteins in 293T cells by Western blotting. HSPA5/BiP/Grp78 and actin were detected as loading controls. C, Distribution of HSP40 members in 293T cells. Ectopically expressed HSP40 proteins were detected by immunofluorescence assay using anti-FLAG antibody. Red and blue signals represent HSP40 proteins and Hoechst33254-stained nuclei, respectively. D, Inhibition of HIV-1 production by HSP40 proteins. Viral production from 293T cells cotransfected with proviral DNA and HSP40 expression vectors was measured by ELISA for p24<sup>CA</sup> antigen and normalized against the untransfected control. Data represent the average and SD from 5 or 6 independent experiments. Asterisk shows the statistical significance ( $P < 0.001$ ) of each measurement versus control. E, The replicative efficacies of AdV, HSV-1, and VV in cells ectopically expressing HSP40 proteins were measured by reporter gene expression. Expression of LacZ in cells ectopically expressing HSP40 proteins was also assessed. Representative data from 2 or 3 independent experiments are shown. Asterisk represents the statistical significance ( $P < 0.01$ ) of each measurement versus control.

B6 (Fig. 3B). These data indicate that HSP40A1 and B6 have profound negative effects on HIV-1 replication.

The data reported above suggest that HSP40s target the production phase of HIV-1's life cycle. We also tested whether HSP40s influence the entry phase in T cells. MT-4 cells constitutively expressing HSP40A1 and B6 were infected with HIV-1 vector pseudotyped with VSV-G bearing an expression cassette for firefly luciferase. The efficiencies of HIV-1 infection in these cells were indistinguishable from those of control cells. As a control, we examined the infection efficiency of an MLV vector pseudotyped with VSV-G bearing a firefly luciferase expression cassette. The efficiencies of MLV infection in these cells were not significantly affected (Fig. 3C). These data suggest that HSP40 proteins primarily limit HIV-1 replication by targeting the production phase, not the entry phase.

## Reduction of HIV-1 RNA Accumulation Through the Inhibition of Rev by HSP40s

Next, we investigated the molecular mechanism underlying the inhibition of HIV-1 production by HSP40s. Expression levels of viral protein in virus-producing cells were decreased (Figs. 2C, D). Therefore, we examined viral mRNA levels in 293T cells cotransfected with proviral DNA and HSP40 expression vectors. The levels of viral transcripts represented by Vpr mRNA were decreased when HSP40A1 or B6 were expressed (Fig. 4A). In contrast, such effects were not observed on GAPDH mRNA. The reductions in the levels of viral transcript were comparable with the reduction of viral production reflected by p24<sup>CA</sup> ELISA (Figs. 1D and 2E, F), suggesting that the inhibition of viral production was due to decreased levels of